EXPLORING THE LIMITS OF UNSATURATED SOIL MECHANICS: THE BEHAVIOR OF COARSE GRANULAR SOIL AND ROCKFILL

The Eleventh Spencer J. Buchanan Lecture

By

Eduardo ALONSO

Friday November 21, 2003

College Station Hilton
810 University Drive
College Station, TX 77840 USA

http://ceprofs.tamu.edu/briaud/buchanan.htm

SPENCER J. BUCHANAN, SR.

Spencer J. Buchanan, Sr. was born in 1904 in Yoakum, Texas. He graduated from Texas A&M University with a degree in Civil Engineering in 1926, and earned graduate and professional degrees from the Massachusetts Institute of Technology and Texas A&M University.

He held the rank of Brigadier General in the U.S. Army Reserve, (Ret.), and organized the 420th Engineer Brigade in Bryan-College Station, which was the only such unit in the Southwest when it was created. During World War II, he served the U.S. Army Corps of Engineers as an airfield engineer in both the U.S. and throughout the islands of the Pacific Combat Theater. Later, he served as a pavement consultant to the U.S. Air Force and during the Korean War he served in this capacity at numerous forward airfields in the combat zone. He held numerous military decorations including the Silver Star.

He was founder and Chief of the Soil Mechanics Division of the U.S. Army Waterways Experiment Station in 1932, and also served as Chief of the Soil Mechanics Branch of the Mississippi River Commission, both being Vicksburg, Mississippi.

Professor Buchanan also founded the Soil Mechanics Division of the Department of Civil Engineering at Texas A&M University in 1946. He held the title of Distinguished Professor of Soil Mechanics and Foundation Engineering in that department. He retired from that position in 1969 and was named professor Emeritus. In 1982, he received the College of Engineering Alumni Honor Award from Texas A&M University.

He was the founder and president of Spencer J. Buchanan & Associates, Inc., Consulting Engineers, and Soil Mechanics Incorporated in Bryan, Texas. These firms were involved in numerous major international projects, including twenty-five RAF-USAF airfields in England. They also conducted Air Force funded evaluation of all U.S. Air Training Command airfields in this country. His firm also did foundation investigations for downtown expressway systems in Milwaukee, Wisconsin, St. Paul, Minnesota; Lake Charles, Louisiana; Dayton, Ohio, and on Interstate Highways across Louisiana. Mr. Buchanan did consulting work for the Exxon Corporation, Dow Chemical Company, Conoco, Monsanto, and others.

Professor Buchanan was active in the Bryan Rotary Club, Sigma Alpha Epsilon Fraternity, Tau Beta Pi, Phi Kappa Phi, Chi Epsilon, served as faculty advisor to the Student Chapter of the American Society of Civil Engineers, and was a Fellow of the Society of American Military Engineers. In 1979 he received the award for Outstanding Service from the American Society of Civil Engineers.

Professor Buchanan was a participant in every International Conference on Soil Mechanics and Foundation Engineering since 1936. He served as a general chairman of the International Research and Engineering Conferences on Expansive Clay Soils at Texas A&M University, which were held in 1965 and 1969.

Spencer J. Buchanan, Sr., was considered a world leader in geotechnical engineering, a Distinguished Texas A&M Professor, and one of the founders of the Bryan Boy's Club. He died on February 4, 1982, at the age of 78, in a Houston hospital after an illness, which lasted several months.

The Spencer J. Buchanan '26 Chair in Civil Engineering

The College of Engineering and the Department of Civil Engineering gratefully recognize the generosity of the following individuals, corporations, foundations, and organizations for their part in helping to establish the Spencer J. Buchanan '26 Professorship in Civil Engineering. Created in 1992 to honor a world leader in soil mechanics and foundation engineering, as well as a distinguished Texas A&M University professor, the Buchanan Professorship supports a wide range of enriched educational activities in civil and geotechnical engineering. In 2002, this professorship became the Spencer J. Buchanan '26 Chair in Civil Engineering.

Founding Donor

C. Darrow Hooper '53

Benefactors   ($5,000+)

ETTL Engineering and Consulting Inc.
Douglas E. Flatt '53

Patrons   ($1,000 - $4,999)

Dionel E. Aviles '53
Aviles Engineering Corporation
Willy F. Bohlmann, Jr. '50
Mark W. Buchanan
The Dow Chemical Company Foundation
Wayne A. Dunlap '52
Br. Gen. John C.B. Elliott
Perry G. Hector '54
James D. Murff '70
Donald E. Ray '68
Spencer Buchanan Associates, Inc.
L. Anthony Wolfskill '53

Fellows   ($500 - $999)

John R. Birdwell '53
Joe L. Cooper '56

Harvey J. Haas '59
Conrad S. Hinshaw '39
O'Malley & Clay, Inc.
Robert S. Patton '61
R.R. & Shirley Bryan
Alton T. Tyler '44

Members ($100 - $499)

Adams Consulting Engineers, Inc.
Demetrios A. Armenakis '58
Eli F. Baker '47
B.E. Beecroft '51
Fred J. Benson '36
G.R. Birdwell Corporation, Inc.
Craig C. Brown '75
Donald N. Brown '43
Ronald C. Catchings '65
Ralph W. Clement '57
Coastal Bend Engineering Association
John W. Cooper III '46
George W. Cox '35
Murray A. Crutcher '74
Dodd Geotechnical Engineering
Donald D. Dunlap '58
Edmond L. Faust '47
David T. Finley '82
Charles B. Foster, Jr. '38
Benjamin D. Franklin '57
Thomas E. Frazier '77
William F. Gibson '59
Cosmo F. Guido '44
Joe G. Hanover '40
John L. Hermon '63
William and Mary Holland
W. Ronald Hudson '54
W.R. Hudson Engineering
Homer A. Hunter '25
Iyllis Lee Hutchin
Mr. & Mrs. Walter J. Hutchin '47
Mary Kay Jackson '83
Hubert O. Johnson, Jr. '41
Lt. Col. William T. Johnson, Jr. '50
Homer C. Keeter, Jr. '47
Richard W. Kistner '65
Charles M. Kitchell, Jr. '51

Mr. & Mrs. Donald Klinzing
Andrew & Bobbie Layman
Mr. & Mrs. W.A. Leaterhman, Jr.
F. Lane Lynch '60
Charles McGinnis '49
Jes D. McIver '51
Charles B. McKerall, Jr. '50
Morrison-Knudsen Co.,Inc.
Jack R. Nickel '68
Roy E. Olson
Nicholas Paraska '47
Daniel E. Pickett '63
Pickett-Jacobs Consultants, Inc.
Richard C. Pierce '51
Robert J. Province '60
David B. Richardson '76
David E. Roberts '61
Walter E. Ruff '46
Weldon Jerrell Sartor '58
Charles S. Skillman, Jr. '52
Soil Drilling Services
Louis L. Stuart, Jr. '52
Ronald G. Tolson, Jr. '60
Hershel G. Truelove '52
Mr. & Mrs. Thurman Wathen
Ronald D. Wells '70
Andrew L. Williams, Jr. '50
Dr. & Mrs. James T.P. Yao

Associates   ($25 - $99)

Mr. & Mrs. John Paul Abbott
Charles A. Arnold '55
Bayshore Surveying Instrument Co.
Carl F. Braunig, Jr. '45
Mrs. E.D. Brewster
Norman J. Brown ' 49
Mr. & Mrs. Stewart E. Brown
Robert P. Broussard
John Buxton '55
Caldwell Jewelers
Lawrence & Margaret Cecil
Howard T. Chang '42
Mrs. Lucille Hearon Chipley
Caroline R. Crompton

Mr. & Mrs. Joseph R. Compton
Harry & Josephine Coyle
Robert J. Creel '53
Robert E. Crosser '49
O Dexter Dabbs
Guy & Mary Bell Davis
Robert & Stephanie Donaho
Mr. Charles A. Drabek
Stanley A. Duitscher '55
Mr. & Mrs. Nelson D. Durst
George H. Ewing '46
Edmond & Virginia Faust
First City National Bank of Bryan
Neil E. Fisher '75
Peter C. Forster '63
Mr. & Mrs. Albert R. Frankson
Maj. Gen Guy & Margaret Goddard
John E. Goin '68
Mr. & Mrs. Dick B. Granger
Howard J. Guba '63
James & Doris Hannigan
Scott W. Holman III '80
Lee R. Howard '52
Mrs. Jack Howell
Col. Robert & Carolyn Hughes
William V. Jacobs '73
Ronald S. Jary '65
Mr. Shoudong Jian '01
Richard & Earlene G. Jones
Stanley R. Kelley '47
Elmer E. Kilgore '54
Kenneth W. Kindle '57
Tom B. King
Walter A. Klein '60
Kenneth W. Korb '67
Dr. & Mrs. George W. Kunze
Larry K. Laengrich '86
Monroe A. Landry '50
Lawrence & Margaret Laurion
Mr. & Mrs. Charles A Lawler
Mrs. John M. Lawrence, Jr.
Jack & Lucille Newby
Lockwood, Andrews, & Newman, Inc.
Robert & Marilyn Lytton
Linwood E. Lufkin '63
W.T. McDonald

James & Maria McPhail
Mr. & Mrs. Clifford A. Miller
Minann, Inc.
Mr. & Mrs. J. Louis Odle
Leo Odom
Mr. & Mrs. Bookman Peters
Charles W. Pressley, Jr. '47
Mr. & Mrs. D.T. Rainey
Maj. Gen. & Mrs. Andy Rollins and J. Jack Rollins
Mr. & Mrs. J.D. Rollins, Jr.
Mr. & Mrs. John M. Rollins
Allen D. Rooke, Jr. '46
Paul D. Rushing '60
S.K. Engineering
Schrickel, Rollins & Associates, Inc.
William & Mildred H. Shull
Milbourn L. Smith
Southwestern Laboratories
Mr. & Mrs. Homer C. Spear
Robert F. Stiles '79
Mr. & Mrs. Robert L. Thiele, Jr.
W.J. & Mary Lea Turnbull
Mr. & Mrs. John R. Tushek
Edward Varlea '88
Constance H. Wakefield
Troy & Marion Wakefield
Mr. & Mrs. Allister M. Waldrop
Kenneth C. Walker '78
Robert R. Werner '57
William M. Wolf, Jr. '65
John S. Yankey III '66
H.T. Youens, Sr.
William K. Zickler '83
Ronald P. Zunker '62

Every effort was made to ensure the accuracy of this list. If you feel there is an error, please contact the Engineering Development Office at 979-845-5113. A pledge card is enclosed on the last page for potential contributions.

Spencer J. Buchanan Lecture Series

1993   Ralph B. Peck   "The Coming of Age of Soil Mechanics: 1920 - 1970"

1994   G. Geoffrey Meyerhof   "Evolution of Safety Factors and Geotechnical Limit
                                State Design"

1995   James K. Mitchell   "The Role of Soil Mechanics in Environmental
                                Geotechnics"

1996   Delwyn G. Fredlund   "The Emergence of Unsaturated Soil Mechanics"

1997   T. William Lambe   "The Selection of Soil Strength for a Stability Analysis"

1998   John B. Burland   "The Enigma of the Leaning Tower of Pisa"

1999   J. Michael Duncan   "Factors of Safety and Reliability in Geotechnical
                                Engineering"

2000   Harry G. Poulos   "Foundation Settlement Analysis – Practice Versus
                                Research"

2001   Robert D. Holtz   "Geosynthetics for Soil Reinforcement

2002   Arnold Aronowitz   "World Trade Center: Construction, Destruction, and
                                Reconstruction"

2003   Eduardo Alonso   "Exploring the Limits of Unsaturated Soil Mechanics:
                                the Behavior of Coarse Granular Soil and Rockfill"

The text of the lectures and a videotape of the presentations are available by contacting:

Dr. Jean-Louis Briaud
Spencer J. Buchanan '26 Chair Professor
Department of Civil Engineering
Texas A&M University
College Station, TX 77843-3136, USA
Tel: 979-845-3795
Fax: 979-845-6554
e-mail: Briaud@tamu.edu

You may also visit the website http://ceprofs.tamu.edu/briaud/buchanan.htm

AGENDA

The Eleventh Spencer J. Buchanan Lecture
Friday November 21, 2003
College Station Hilton

2:00 p.m.   Welcome by Jean-Louis Briaud

2:05 p.m.   Introduction by Paul Roschke

2:10 p.m.   Introduction of Lymon Reese by Charles Aubeny

2:15 p.m.   "Unique Applications for the Design of Piles under
                   Lateral Loading" Special Lecture by Lymon Reese

3:15 p.m.   Discussion

3:25 p.m.   Introduction of Eduardo Alonso by Jean-Louis Briaud

3:30 p.m.   "Exploring the Limits of Unsaturated Soil Mechanics: the
                   Behavior of Coarse Granular Soil and Rockfill"
                   2003 Buchanan Lecture by Eduardo Alonso

4:30 p.m.   Discussion with Darrow Hooper

4:40 p.m.   Closure with Phillip Buchanan

5:00 p.m.   Photos followed by a reception at the home of Jean-Louis
                   and Janet Briaud.

Professor Eduardo ALONSO

Professor Eduardo Alonso is Professor of Geotechnical Engineering at the Escuela Técnica Superior de Ingenieros de Caminos Canales y Puertos, Universidad Politécnica de Catalunya, in Barcelona, Spain. Born in 1947, he received his Engineering degree from the Universidad de Madrid in 1969 and his PhD from Northwestern University in 1973.

His main topics of interest are reliability and risk in geotechnical engineering, behaviour of partially saturated soils, expansive soils and rocks, numerical analysis of geotechnical problems (soils and rocks), field measurements and geotechnical backnalysis, slope stability. He has been involved in over ninety consulting jobs in Spain and abroad involving deep excavations, nuclear power stations, diaphragm walls, ground improvement techniques, design of shallow and deep foundations, slope stability, underpinning of structures, site investigation reports, breakwaters, concrete and earth dams and tunnels.

Professor Alonso has written over 250 papers published in National and International Symposia, specialized research books, and learned journals. Among his most prestigious awards are the Telford Medal from the Institution of Civil Engineers in the United Kingdom, the Premio Jose Toran from the Comite Espanol de Grandes Presas in Spain, and the Conference Coulomb from the Comite Francais de Mecanique des Sols in France. He is truly an internationally known engineer and chairs the ISSMGE Technical Committee TC6 on Unsaturated Soils. In 1995, he was elected to the Royal Academy of Engineering of Spain.

Professor Eduardo Alonso delivered the eleventh Spencer J. Buchanan Lecture on November 10, 2003 at the Hilton Hotel in College Station, home of Texas A&M University. The topic of his lecture was "Exploring the Limits of Unsaturated Soil Mechanics: The Behavior of Coarse Granular Soil and Rockfill".

EXPLORING THE LIMITS OF UNSATURATED SOIL MECHANICS: THE BEHAVIOUR OF COARSE GRANULAR SOIL AND ROCKFILL

E.E. Alonso

Department of Geotechnical Engineering and Geosciences

Universitat Politècnica de Catalunya

Gran Capitán s/n, Módulo D-2

Barcelona 08034

SPAIN

Tel: 34 93 4016866, Fax: 34 93 4017251, e-mail: eduardo.alonso@upc.es

Date paper written: November 1st 2003

EXPLORING THE LIMITS OF UNSATURATED SOIL MECHANICS: THE BEHAVIOUR OF COARSE GRANULAR SOIL AND ROCKFILL

− Eduardo Alonso

Department of Geotechnical Engineering, UPC, Barcelona (Spain)

1 INTRODUCTION

A large variety of engineering situations require, for a proper understanding of underlying basic mechanisms of soil deformation, the contribution of unsaturated soil mechanics. A common and distinctive feature of situations involving unsaturated soils is that the triggering mechanism for soil deformation and, eventually, soil failure, is the environmentally induced change in water content. These external actions result in change degrees of saturation or, at least, in the generation of negative pore water pressure. A useful preliminary ordering of the kind of problems, which may have their origin in environmentally-controlled changes in water content, may be based on the classical classification of soils. Consider the following set of real cases, ordered in view of the plasticity and grain size distribution of the soil involved:

High plasticity expansive barriers for waste isolation. A frequently proposed scheme for radioactive waste disposal in Europe and Japan is to isolate the nuclear canisters by means of rings of compacted and initially unsaturated bentonite. The canister space is filled with highly expansive blocks of compacted bentonite, which will swell as water percolating from the host rock hydrates the clay. Very high swelling pressures (6-7 MPa), essentially controlled by the initial porosity of the bentonite, are expected in this case. A description of the kind of phenomena present in this case and the procedure to simulate the behaviour of these highly impervious and highly swelling barriers may be found in Gens et al (1998). Swelling and shrinkage is dominated by the hydration phenomena of clay particles and clay aggregates

Foundations on natural expansive medium to high plasticity clays. This is a classical example, which has received considerable attention over decades in different geographical areas characterised by arid climates (which explain the strong relative humidity changes in the exposed foundation soils) and high plasticity clays (Nelson and Miller, 1992). The series of International Conferences on Expansive Soils and, in recent times, the International Conferences on Unsaturated Soils (Paris, 1995; Beijing, 1998; Recife, 2002) offer real cases, experimental and theoretical research. Although swelling is the dominant feature, a joint collapse –swelling behaviour may be expected in some cases. A discussion of this dual behaviour is given in Alonso, Gens and Hight (1987). The microstructure of unsaturated clays offers a physical explanation for the observed behaviour. Swelling/shrinkage is

associated with clay aggregates but capillary phenomena control the "large scale" geometrical arrangements of clay aggregates and coarser particles (Gens and Alonso, 1992). These soils have typically a bi-modal distribution of pore sizes.

Embankments in low to medium plasticity silts and sandy clays. It is well known that the expected volume change of these materials upon wetting will be controlled by the initial density and water content. As a rough approximation for compacted soils, densities and water contents below the Normal Proctor Optimum mark the beginning of the risk of collapse in practice. Densities at the Modified Proctor Optimum and above may lead to swelling. The behaviour of embankments after construction offer a very good source of field data. As in the previous case the particular soil microstructure and the dominant clay minerals explain the role of suction.

Sands. No significant applied case involving unsaturated sands has been found in the author's experience. Laboratory experiments involving unsaturated fine to medium sands indicate that expected deformations under wetting-drying cycles are very small, even if the sand has a low density. Figure 1b shows collapse strains measured in a low density (e = 0.95) uniform sand (grain size is shown in Figure 1a) as a function of vertical stress, when suction was decreased from the initial value (a high value corresponding to a Relative Humidity of 56%) to the low suctions shown in the figure (Alonso and Romero, 2003). The case marked s = 0 corresponds to a fully saturated specimen. Even for this very low density, the maximum measured collapse strain is around 0.65%. If a minimum compaction is given to this sand, volumetric strains would be reduced to negligible values. Note also in Figure 1b that the application of confining stresses in excess of 70 kPa eliminates also the risk of strain deformations upon saturation.
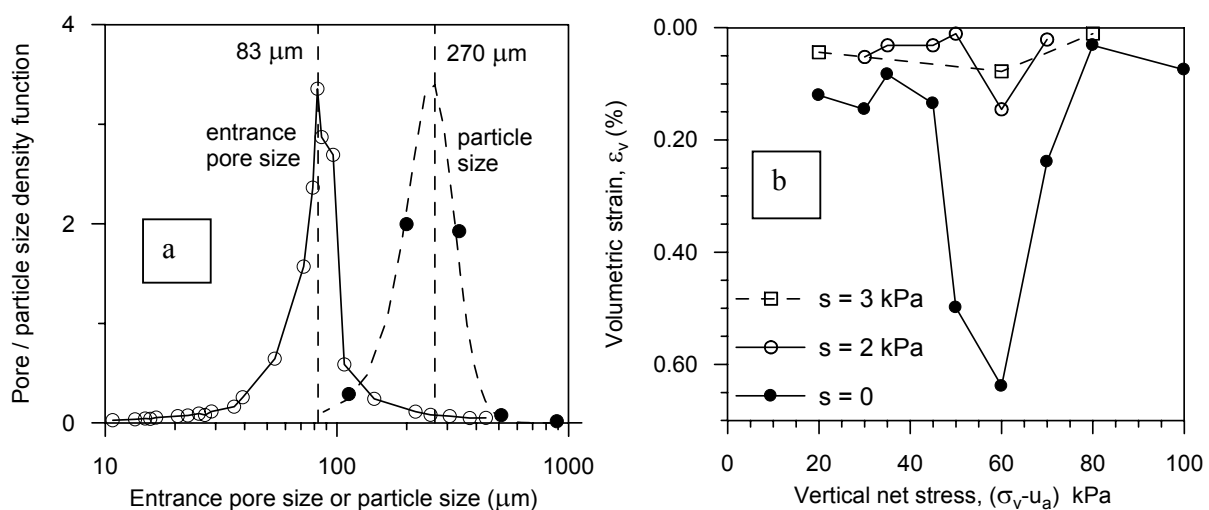

Figure 1. Beach sand from Castelldefels. a. Grain and pore size distribution. b. Collapse observed in suction controlled wetting under load tests.

It is accepted that the behaviour of unsaturated sand is controlled by capillary effects. The relevant suction in this case is the matric suction. Numerical experiments performed on granular aggregates of spherical particles bonded by capillary menisci are able to reproduce the experimental observations (Figure 2; Gili and Alonso, 2002).
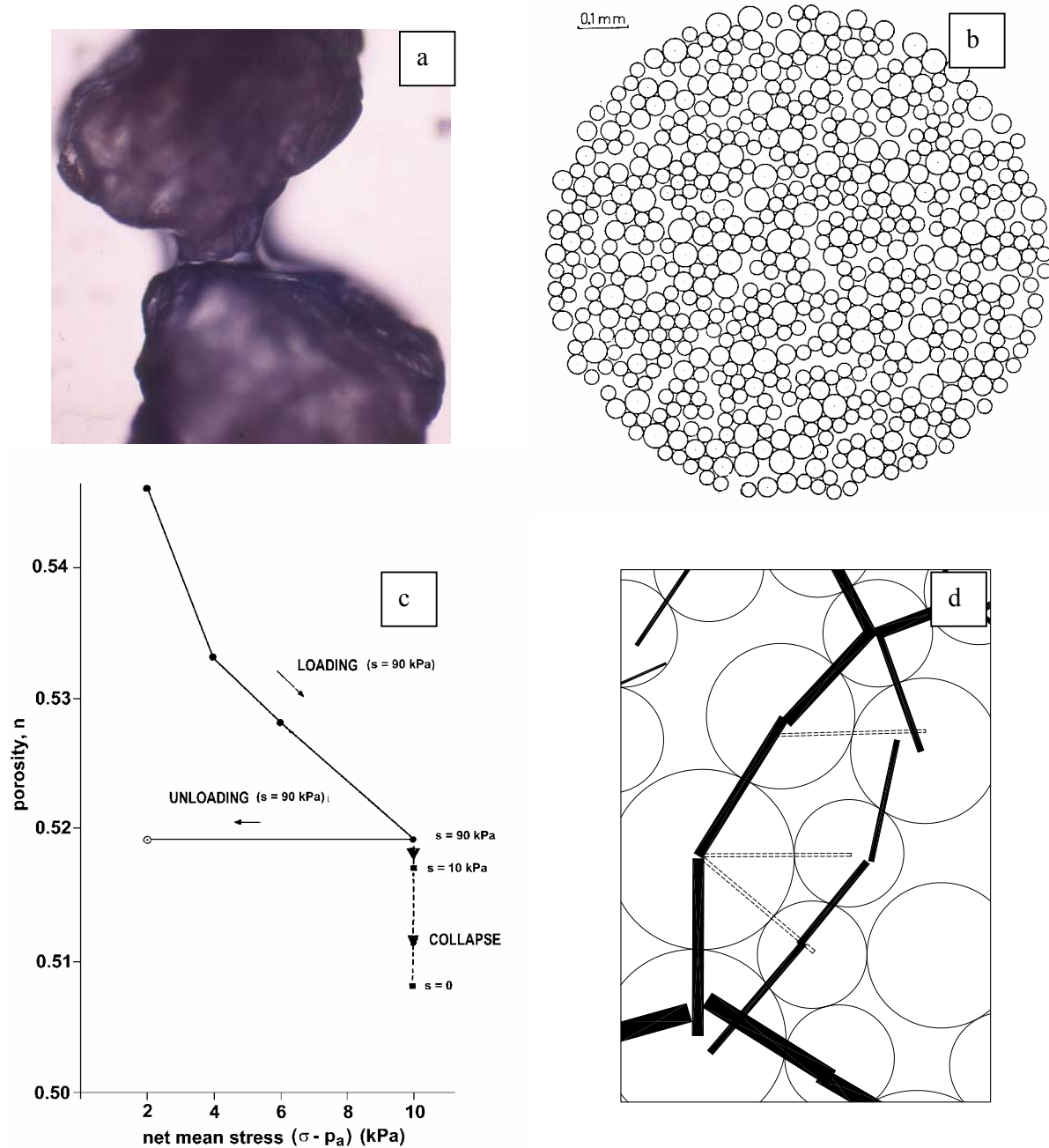

Figure 2. Numerical experiments on ideal aggregates of spherical particles. a: Water meniscus between two sand grains.b: Arrangement of spherical particles. c: Results of a loading-collapse simulation. d: Stabilizing effect of menisci allows the configuration of a double force chain.

It was shown that the menisci at the grain-to-grain contacts help to maintain stables the force chains that develop in the loaded granular structure. This effect may be described as an internal tensioning, which adds stability and prevents buckling of loaded chains. When suction is reduced some force chains are destroyed and a rearrangement of the soil structure takes place. This is the nature of wetting induced collapse.

The above experimental results and numerical simulations refer to fine sands and silts. When the size of the particles increase it is difficult to explain collapse on the basis of this mechanism because the intensity of the capillary forces become very small if compared with intergranular forces resulting from self weight and external loading. Yet, the field experience shows that rockfill dams and rockfill embankments experience significant settlements when they are wetted. The purpose of this paper is to explore these phenomena, to provide a physical explanation to experimental observations and to present a suitable model, which may be used to simulate the observed behaviour of rockfill embankments.

2 VOLUMETRIC DEFORMATIONS OF ROCKFILL

It was implicit in the previous presentation of sand and silt behaviour that capillary forces increase the contact forces between grains and therefore they contribute to soil stiffness and strength. Consider, in Figure 3a the attraction force between two spherical particles induced by a common meniscus. The attraction force, F_w, was computed using some theoretical results (see Gili and Alonso, 2002; Gili, 1988) for menisci of thoroidal shape. In the four cases represented ("Rockfill": diameter D=50 cm, "Gravel": D=10 mm, "Medium sand": D=0.5 mm, "Medium silt": D=0.01 mm), the weight of the solid particle is used to normalize the value of F_w. For sizes in excess of gravel the grain weight is significantly higher than the maximum capillary force at the grain to grain contacts. Therefore, for coarse granular particles internal forces of capillary nature will tend to be negligible. Additional information in this regard is provided in Figure 3b where the absolute value of the capillary forces is interpreted in terms of internal inter-granular stresses. For this interpretation a cubic configuration of spheres is adopted. The calculated stress is computed as the averaged force on a reference plane through the contacts between two parallel layers of spheres. The reduction of the number of contact forces, per unit area, as the size of particles increases explains the weak capillary stresses computed for coarse granular aggregates.

It is concluded that capillary effects can hardly explain the observed volume changes in rockfill embankments and dams. However, there is widespread field evidence which shows that wetting may induce large settlements in rockfill structures. This is a well-known phenomenon which has received a continuous interest ever since the widespread use of rockfill in dams and, more particularly, since the beginning of the 20th Century. In large earth and rockfill dams rapid

"collapse" settlements have been associated with water impoundment. It was also soon realized that wet compaction reduced notably collapse settlements as well as the rate of settlement development in time (Sherard and Cooke, 1987).

The first impoundment leads usually to the maximum collapse settlements. However, strong rainfalls may also contribute to significant volumetric deformations during the early life of dams. Figure 4 shows a representative cross section of El Infiernillo dam in Mexico and the records of vertical and horizontal movements measured at some surface marks (Marsal, 1973; Marsal et al, 1976). The dam has a central clay core and large conglomerate and diorite rockfill shells which were dumped in place without watering. The deformation record for Mark M-10 shows the collapse of the upstream shell during the first impoundment in 1964. After a period of 18 months (Jan 1965 to July 1966) in which the rate of deformation decreased steadily, a rapid increase of settlements and horizontal deformations is observed in Marks M-10 and M-21. This increased rate of deformation is visible until the end of 1968 and it corresponds to a period of heavier rainfall which started in 1966.
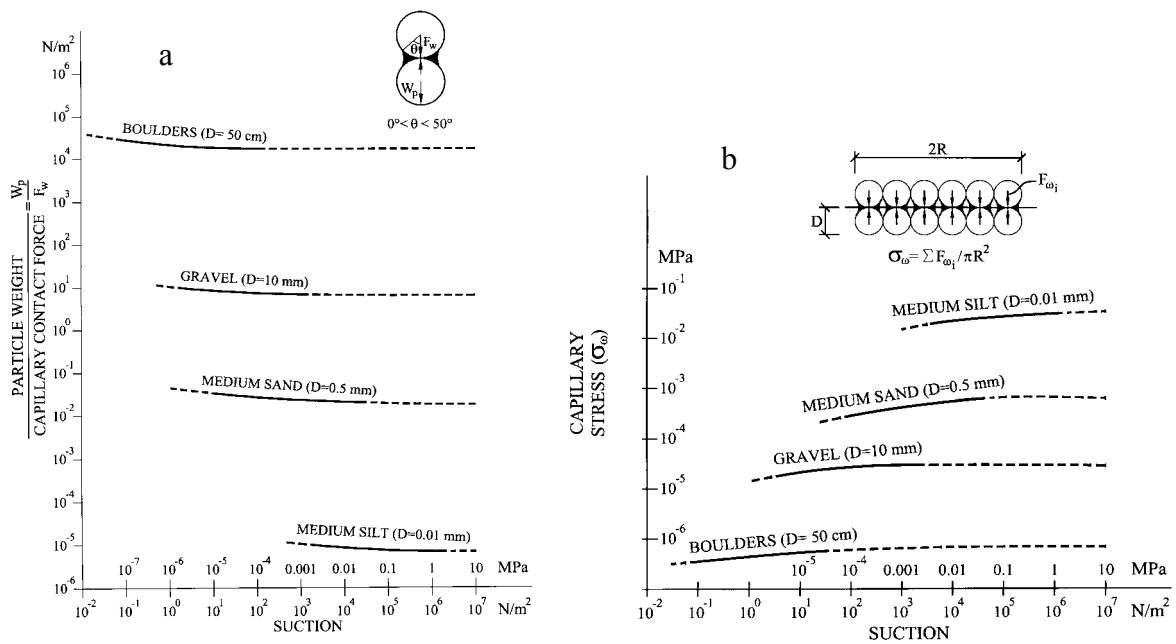

- Figure 3. Simple capillary model for spheres in contact. a: Normalized attraction force between two spheres. b: Capillary stresses for a cubic arrangement

Unlike dam shells, embankments for roads and railways are rarely flooded. But they are exposed to rainfall and therefore one should expect a similar behaviour to the observations in El Infiernillo (and, in fact, in most rockfill dams). Soriano and Sánchez (1999) have described the behaviour after construction of several shale and schist embankments belonging to the high speed railway line linking Madrid and Sevilla in Spain. One of the cases described which corresponds to a 40m high rockfill embankment is illustrated in Figure 5. There is a clear correlation in this case between

rainfall intensity and rate of settlement during the period 1993-1998. It is interesting to realise that the rainfalls at the end of 1997, having an intensity similar to the rainfalls recorded at the end of 1996 did not result in additional settlements.
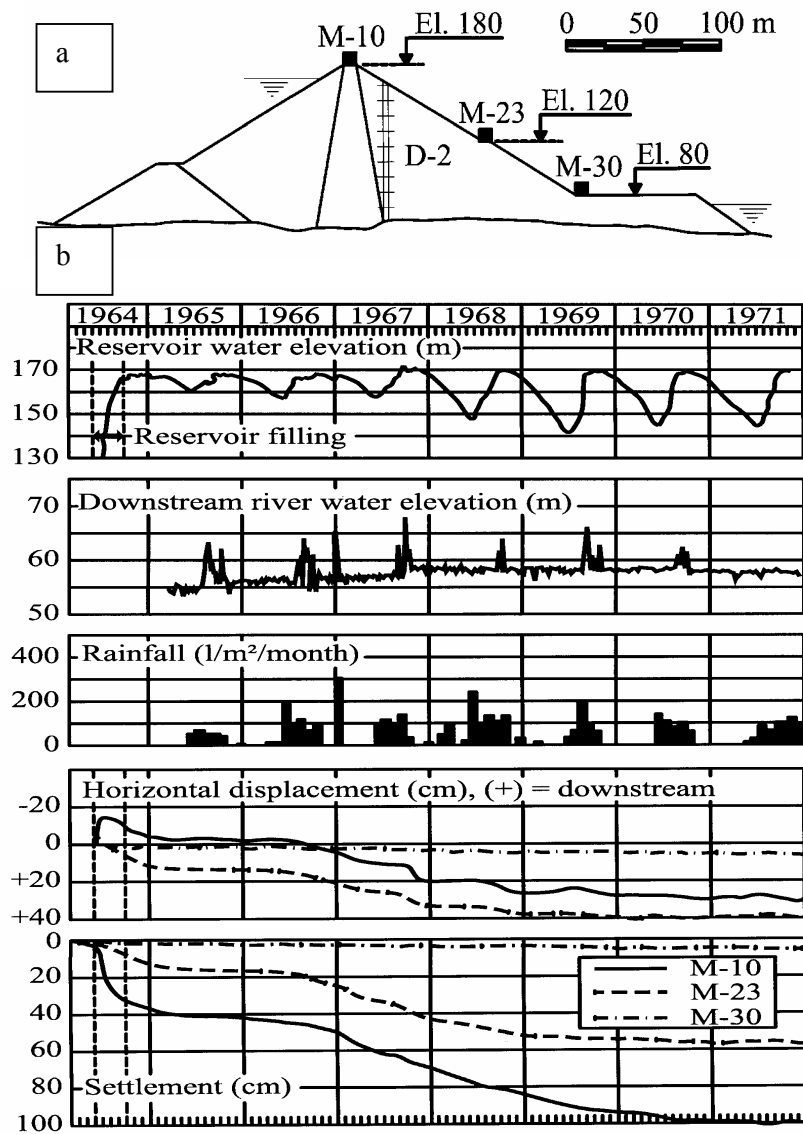
- Figure 4 .a: Infiernillo dam, Mexico. b: Settlements and horizontal displacements observed in topographic marks. (Marsal et al, 1976)
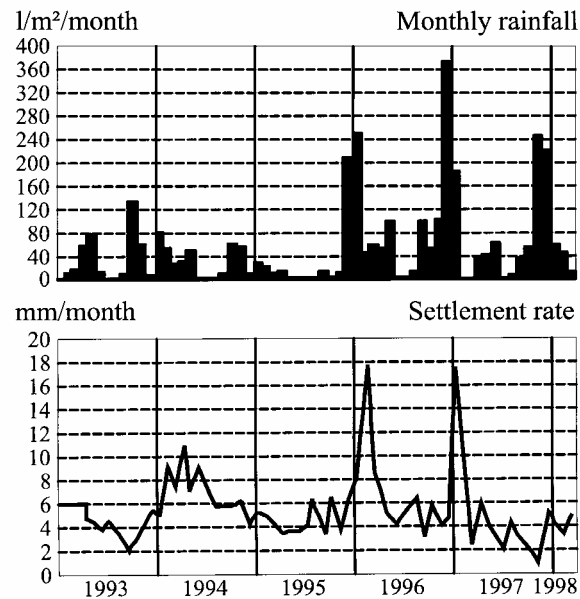
Figure 5. Settlement rates of a 40 m high shale embankment belonging to the high speed railway line between Madrid and Sevilla and rainfall records in the area (Data provided in Soriano and Sánchez, 1999)

Collapse phenomena of coarse granular aggregates have been observed in dams, embankments but also in the Laboratory (Sowers et al, 1965, Marsal, 1973, Nobari and Duncan, 1972) when testing specimens of compacted gravel. Compression tests performed by several authors (Sowers et al, 1965; Marsal, 1973; Clements, 1981) on rock wedges compressed against surfaces of the same or different material suggest that the breakage of wedge the contact area is the main mechanism which explains the deformation of rockfill as well as the effect of water. Figure 2.4 shows the compression test reported by Clements (1981) on a rock wedge having a point solid angle of 169.1°. Saturation of the wedge tip, two hours after the application of the compression load results in a sudden acceleration of deformations. Terzaghi (1960) was one of the first to suggest that rockfill deformations are induced by the breakage of particles in the proximity of highly stressed contact points and the subsequent reorganization of the granular structure towards a stable configuration. The presence of water implies an acceleration of the contact breakage and therefore of the global deformation of the granular material. These phenomena are further discussed in the next section

3   SUBCRITICAL CRACK PROPAGATION AND PARTICLE FAILURE

Various phenomena have been proposed to explain the reduction of rock strength due to the water action: the loss of cohesion due to the reduction of surface energy of minerals (Vutukuri and Lama, 1978); suction reduction (Vutukuri and Lama, 1978); the expansion of clay minerals (De Alba and Sesana, 1978 ; Delgado et al., 1982). However, it appears that subcritical crack propagation

20

phenomena seem to offer a consistent explanation for the experimental observations.

SHAPED ROCK TIP
$\beta = 169°$

TIME (min)

DISPLACEMENT 10^{-3} (mm)

SATURATION
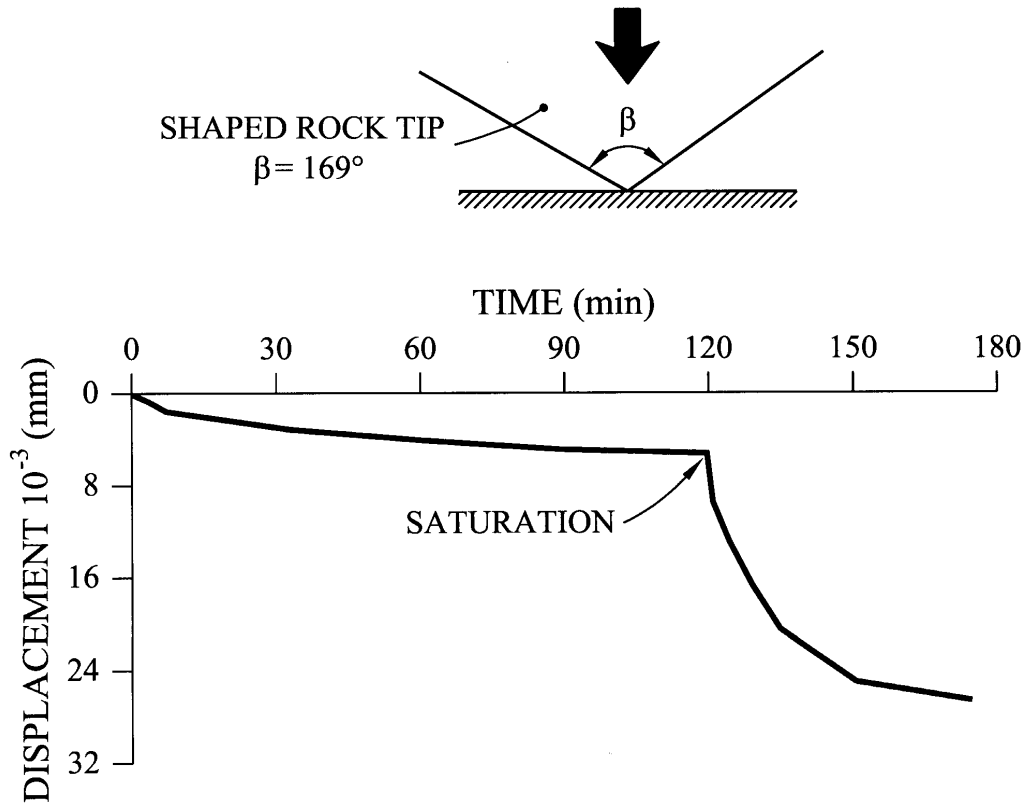
Figure 6. Flooding test of a rock wedge (Clements, 1981)

Within the classical theory of fracture mechanics, the rapid propagation of a crack occurs when the stress intensity factor (K) becomes equal to a critical value (Kc), which is a material parameter (known as toughness). The value of K depends of the geometry of the problem, the loading mode (tension, shearing normal or parallel to the fissure) and of the intensity of the applied stress. For a given loading mode (index L),

$$K_L = \beta \sigma \sqrt{\pi a} \qquad\qquad (1)$$

where a is the length of the fissure, σ, the relevant stress and β is a constant which depends on geometry. A common case is L=I (pure tension).

However, it has been observed that the fracture can propagate at a finite velocity V, even if K < Kc (sub-index L is omitted to simplify). This phenomenon is known as a sub-critical propagation of the fracture. Velocity V depends on the value of K but also on external "corrosive" agents such as water. Stress corrosion research (Michalske et Freiman, 1982; Atkinson et Meredith, 1987) help to interpret the effect of water on fracture propagation. Experimental data, such as the test results shown in Figure 7, show that V depends on K and on the Relative Humidity (RH) of the

21

atmosphere, in which the tests are performed. Relative Humidity is defined as the ratio p_v/p_v^0, where p_v^0 is the saturation pressure of vapour at temperature T and p_v the current value of vapour pressure in the atmosphere. Theoretical results (Widerhorn et al, 1980,1982 ; Freiman, 1984) show the structure of the relationship between V and K and RH:

$$V = V_o.(RH).\exp\left[-\left(E^{\overset{+}{+}} - bK\right)/RT\right] \tag{2}$$

Term ($E^{\overset{+}{+}}$-bK) is interpreted as an activation energy of the corrosion reaction.. $E^{\overset{+}{+}}$ incorporates the energy terms which do not depend on the stress. The term bK is interpreted as the mechanical work between the initial and the activated states. R is the gas constant and T the absolute temperature. Parameters V_0, $E^{\overset{+}{+}}$ et b are constants for a given environment characterized by T and RH. Equation (2) is consistent with the experimental data presented in Figure 7 and other data on glass and rock fracture presented by Atkinson et Meredith (1987). In all cases it is observed that V increases in direct proportion to the RH. If the crack propagates in a liquid, experiments (Freiman, 1984) indicate that the propagation velocity is proportional to the RH of the air in thermodynamic equilibrium with the liquid.
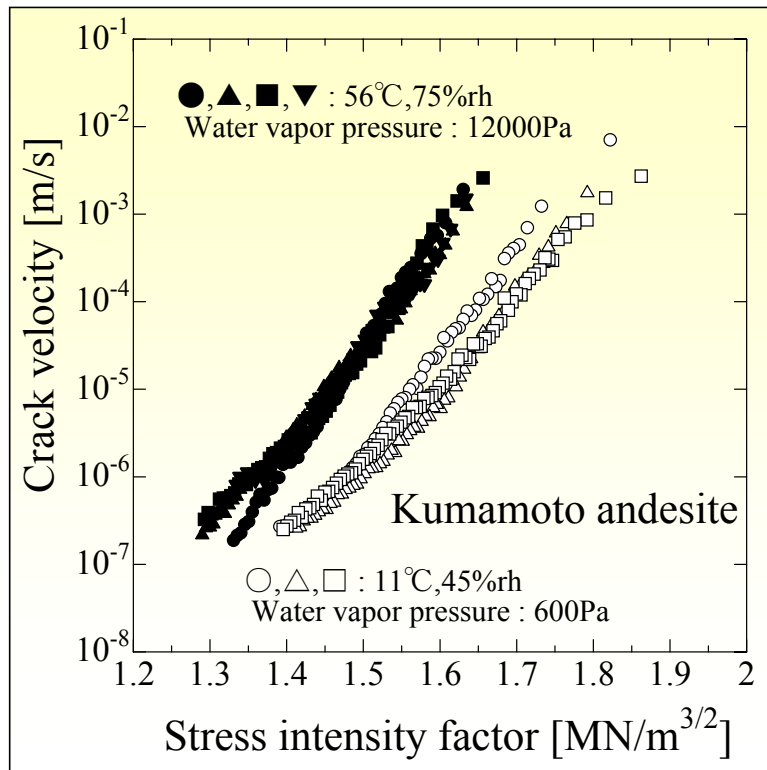
Figure 7. Tests on Kumamoto andesite reported by Nara and Kaneko, 2003
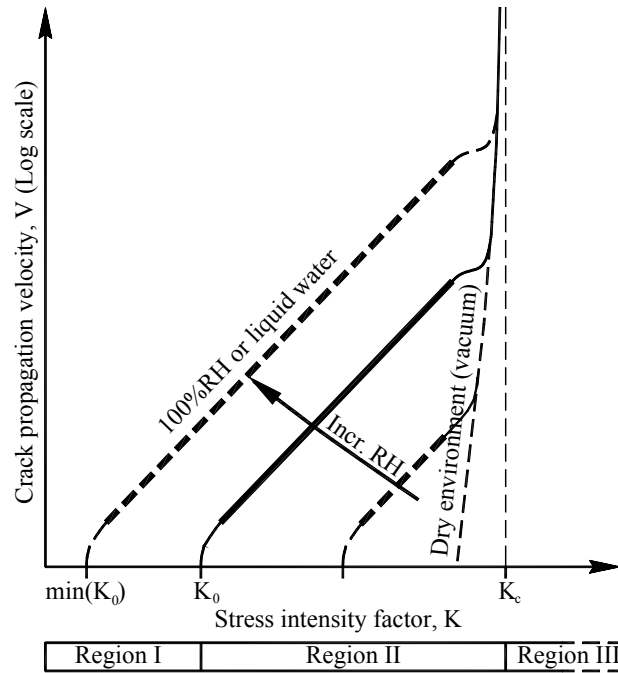
- Figure 8. Schematic subcritical crack growth curves and conceptual model (Alonso & Oldecop, 2000).

In the case of water, Relative Humidity is a procedure to describe its chemical potential or suction. In fact, the psychrometric law establishes,

$$RH = \exp\left[-\frac{M_v(s+\pi)}{RT}\right]$$
(4)

where $\psi = s + \pi$ is the total suction, s is the capillary or matric suction and π, the osmotic suction. M_v is the molar volume of water.

A subcritical crack growth mechanism, as outlined above, was proposed by Alonso & Oldecop (2000) to explain why both time dependent strains and collapse strains, simultaneously depend on the stress state and the water action. A rockfill element can be viewed as composed by a certain number of rock particles, each one containing a large number of micro and macro-cracks. Those cracks will propagate due to the interaction of load and water effects. Every time one of those cracks fails, a particle breakage occurs and hence an increment of strain occurs.

Figure 8 is a schematic representation of actual test data on crack propagation velocity. It will be used to describe in qualitative terms the process of rockfill deformation.. The crack propagation velocity is a function of the applied loads and the water action. Load effects are taken into account by means of the stress intensity factor, K. Water action is conveniently measured by means of the relative humidity measured in the testing environment, i.e. the air surrounding the specimen. The stress intensity factor axis is divided into three regions. Cracks lying in region I ($K<K_0$) do not propagate at all. Hence in a steady state, when the rockfill is not undergoing any deformation, all

cracks contained in the rockfill particles lie in region I. If a load increment is then applied, the K values will move along the K axis. This process will be controlled by the particle geometry, the particular position of each crack and the crack length. Some cracks will fall in region III where the stress intensity factor is greater than the fracture toughness, K_c. Those cracks will fail instantaneously producing the rockfill instantaneous component of strain, as observed in experiments. Other cracks will fall in region II and will grow, with a finite value of the propagation velocity, until they fail. These cracks determine the rockfill time–dependent component of strain.

If the relative humidity is increased, Figure 8 shows that cracks lying in region II will increase their propagation velocity. Moreover, some cracks from region I will move towards region II, due to the reduction in the limit value K_0 as the relative humidity increases. This will produce an additional increment of strain, which is not related to an increment in load, i.e. a collapse deformation.

The proposed conceptual model explains the characteristic behaviour of rockfill and its dependence on loads and water action. According to this model one may conclude that the key parameter which controls the influence of water in the mechanical behaviour of rockfill is the relative humidity measured in the air surrounding the rock particles (provided the gas phase is in thermodynamical equilibrium with the rock particles). The idea was then to perform tests on gravel-like material with relative humidity control.

4   TESTS ON GRAVELS WITH RELATIVE HUMIDITY CONTROL

4.1   Oedometer Tests

Previous considerations led to the idea that performing rockfill mechanical tests under controlled variable moisture conditions would provide information of water action on rockfill compressibility from a new perspective. The RH control technique was first used in geotechnical testing, in unsaturated soils research (Esteban, 1990; Bernier et al, 1997; Delage et al, 1998; Yahia.-Aissa, 1999; Villar, 1999; Romero, 1999; Romero et al, 1999, 2001). In order to apply the technique to rockfill materials, some difficulties should be overcome.

This technique is based on the following physico-chemical principle: if a liquid (i.e., water contained in a soil or rock pore) is allowed to reach equilibrium with its vapour, the partial pressure of vapour, p_v, is related to the matric suction, s, by equation (4)

The sum ($s+\pi$) in equation 4 is called the "total suction", ψ. Eq. 4 implies that, the control of total suction in any specimen kept in a closed system, can be achieved by controlling the RH in the environment surrounding the specimen, provided that enough time is allowed for the system to reach equilibrium. In this technique, water transport is entirely transported through the gas phase, either by advection or by molecular diffusion of water vapour. Therefore, this procedure is also known as the "vapour equilibrium technique".

RH control on the specimen environment can be achieved by introducing a chemical solution within the testing system. The solution is kept in a separate vessel, avoiding direct contact with the specimen but only with the system gas phase. Therefore the RH in the gas phase depends on the temperature, the chemical composition of the solute and the solution concentration. By changing the last two factors, the RH in the testing environment is controlled.

Different test setups are used in a relative humidity control technique. The simplest one consists of enclosing the specimen and the solution in a leak-proof container and allowing time for the system to reach equilibrium. This type of test setup was used for the retention curve assessment of soils and rocks (Romero, 1999; Romero et al, 1999, 2001) and also in oedometer tests on soils (Esteban, 1990). Its fundamental drawback is that equilibration periods are rather long, since all water transfer between solution and specimen has to occur by molecular diffusion. However, this technique was used in the present experimental work for the determination of the retention curve of the tested rock, a slate of Cambric origin, extracted from the Pancrudo River outcrop (Aragón, Spain). The retention curve can be plotted either as suction vs. water content or RH vs. water content, as in Figure 9. In the high RH range (>99%), in which the vapour equilibrium technique becomes inaccurate, the data for the retention curve were obtained by axis translation and tensiometer techniques. The retention curve of the tested rock shows hysteresis effects, a typical behaviour of most porous materials.

An alternative procedure to overcome the problem of long equilibration periods associated with the vapour equilibrium technique is to induce airflow between the solution and the specimen. In this way, water vapour is transported by advection, which is a more efficient transport mechanism than the sole diffusion. In rockfill testing, this procedure can be used with an additional benefit: due to the pressure of large rockfill voids, a relatively large air flow can be passed through the specimen, making water transfer more efficient and hence reducing testing delays.
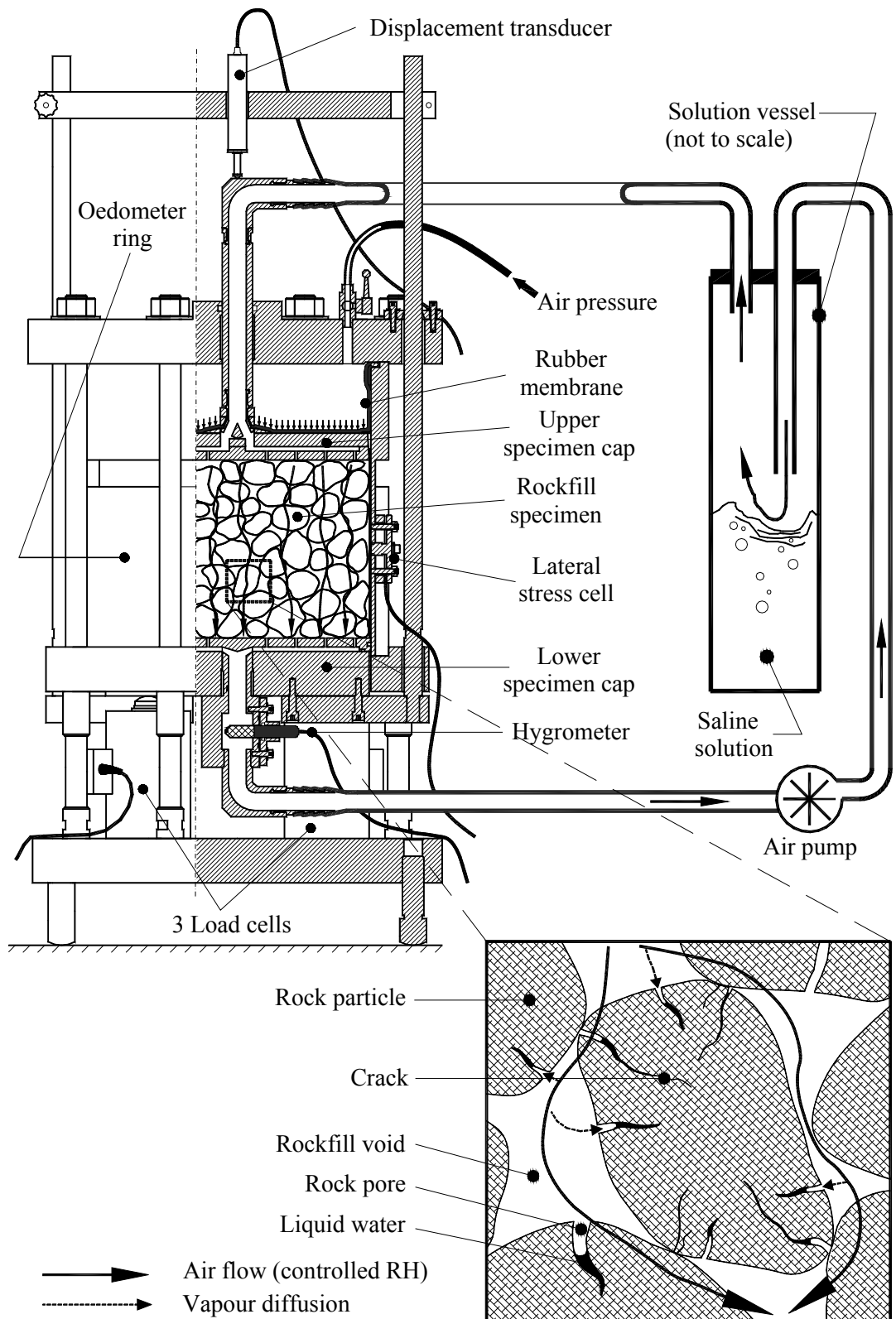
A series of one–dimensional compression test with RH control was performed on specimens of Cambric quartzitic shale (Pancrudo shale). The test setup is shown in Figure 10. A 300 mm diameter oedometer in which the RH of the specimen could be controlled was designed and built. Vertical load was applied by means of air pressure. Vertical load was also measured at the bottom platten by means of three load cells. In this way, friction stresses along the ring wall could be determined. Devices for lateral stress and lateral friction measurement were also incorporated into the oedometer. Airflow was produced in a closed-loop circuit by an electric membrane pump. The air passes through a vessel containing the saline solution and then flows through the rockfill specimen. RH in the airflow is controlled by means of the chemical composition and concentration of the saline solution. A capacitive hygrometer was installed at the specimen outlet in order to get a continuous reading of RH evolution.

25

If the whole system (i.e., specimen + solution vessel + tubing) is leak-proof, the water mass introduced into the specimen during a step of a wetting path (or the mass extracted from the specimen during a drying step) can be measured by successive weightings of the solution vessel.
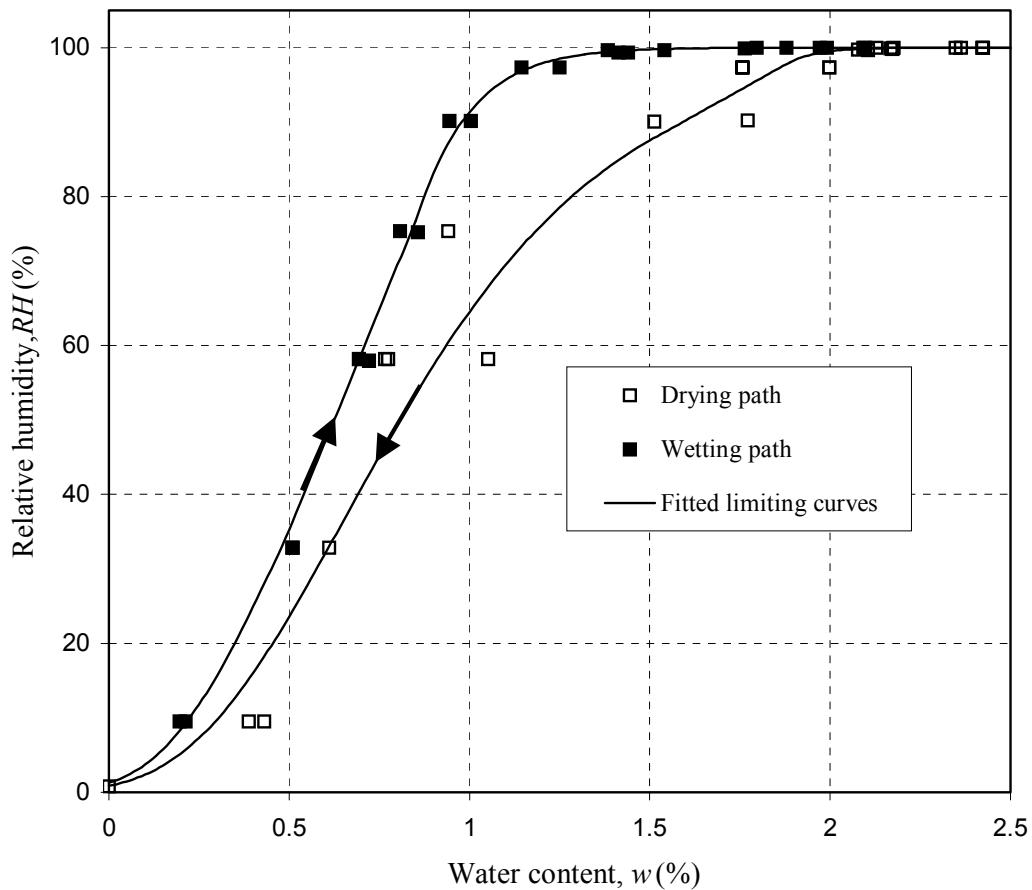
Figure 9. Retention curve for the tested shale rock

Figures 11a and 11b show the paths followed by some of the tests performed (in a vertical stress – total suction space) and the stress-strain behaviour measured in the compacted crushed Pancrudo shale, 40mm in maximum particle size. Each test started in an air-dry condition, which means an initial total suction value close to 100 MPa. The vertical stress was increased in steps, allowing the specimen to deform for at least 1000 minutes under constant stress. Since no steady condition was attained at any load step (in a strain-log(t) type of plot), the strain values used for the stress-strain graphs (Figure 11b) were conventionally defined as the measurement recorded 1000 minutes after the application of the load increment. Total suction changes under constant vertical stress were induced by means of the relative humidity control system both in wetting and drying senses.

26

Displacement transducer

Solution vessel
(not to scale)

Oedometer ring

Air pressure

Rubber membrane

Upper specimen cap

Rockfill specimen

Lateral stress cell

Lower specimen cap

Saline solution

Hygrometer

Air pump

3 Load cells

Rock particle

Crack

Rockfill void

Rock pore

Liquid water

Air flow (controlled RH)

Vapour diffusion

•   Figure 10. Large diameter Oedometer device with RH control and interpretation of vapour diffusion within a rockfill specimen

The features of rockfill suction-dependent behaviour pointed are evident from figure 11. As total suction decreases (wetting), the compressibility increases, up to a maximum value corresponding to the saturated state (ψ = 0 MPa). Within a wide range of strain values, normal compression lines approach a linear strain-stress relationship. Collapse strains are observed to occur upon wetting under constant vertical load (tests 2 and 4). It is also clear from figure 11b that during a short initial stage, under low applied stresses, the described suction-dependent behaviour does not apply, but only beyond a threshold stress value, which will be denoted as σ_y ($\cong$ 0.20 MPa). When $\sigma < \sigma_y$, the sole effect of suction changes is the development of rather moderate swelling/shrinkage strains, but no collapse strains occur upon wetting.

It is shown that the material may attain an even lower compressibility when the specimen is dried beyond the initial "air dry" condition (test 2). A uniqueness of normal compression lines (NCL) for each single total suction value seems well supported by the new experiments. Finally, beyond a certain strain value, the stress-strain relationships are no longer linear, but they become curved with its concavity directed towards the stress axis, i.e. the material stiffens as stress and strain increase. Plotting the same experimental data in a strain-log stress graph (Figure 12) yields the typical shape of Normally Consolidated Lines (NCLs) of granular materials. Isotropic tests performed by Coop and Lee (1995) also showed that NCLs for dry sands lie above those of saturated soils. The present experimental results agree with those early observations and moreover they suggest that the position of NCLs is controlled by total suction.

The type of behaviour shown in figure 12 was interpreted in terms of particle breakage mechanisms by number of authors (Coop and Lee, 1995; Pestana & Whittle, 1995; McDowell & Bolton, 1998). It is widely accepted that during an initial stage, under low applied stresses, deformation occurs due only to particle rearrangement. Moreover, it is assumed that the onset of particle breakage leads to the bend in the NCL, causing the rapid increase of the material compressibility index. Under higher loads, the observed linear strain-log stress NCLs were attributed (McDowell & Bolton, 1998) to the particular features of the particle breakage process, when the grain-size distribution approaches a fractal. McDowell & Bolton (1998) called "clastic yielding" and "clastic hardening" the second and third stages respectively. The same nomenclature will be used in the following.

These micromechanical interpretations are in agreement with the present experimental observations, when considered in the framework of the conceptual model proposed by Oldecop and Alonso (2001). The water-dependent features of rockfill mechanical behaviour are supposed to occur due to fracture propagation phenomena. Hence, such dependence would occur only when particle breakage takes place, i.e. during clastic yielding and clastic hardening stages. Since no particle breakage occurs during the particle rearrangement stage, no water dependence should be expected, which is indeed what follows from the experimental data in figure 11 and 12.
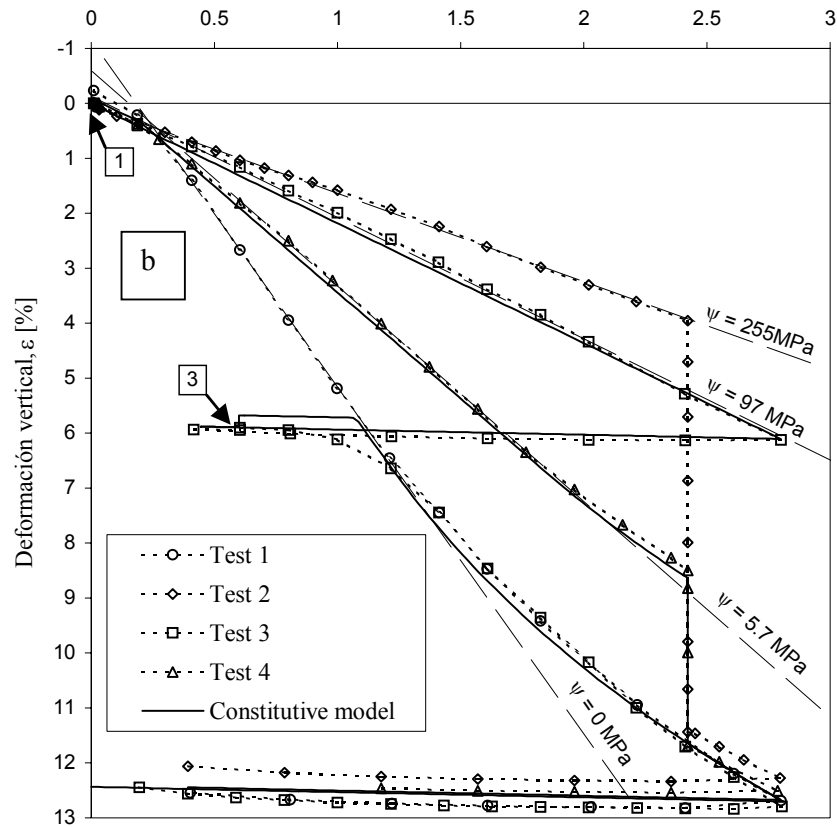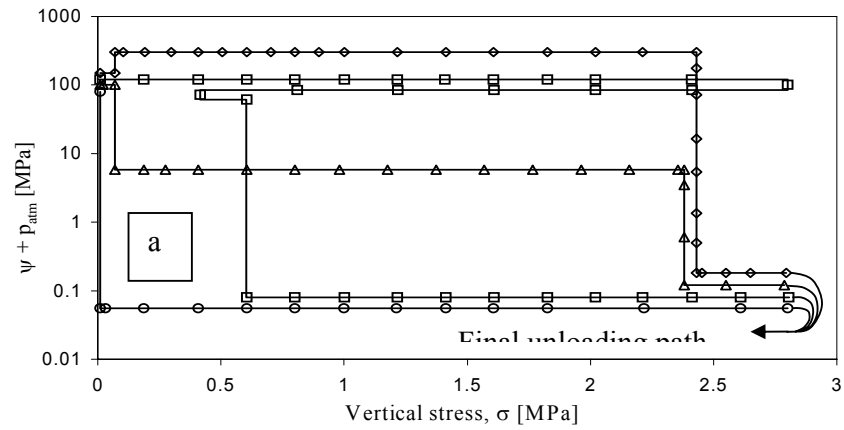
Figure 11. a: Loading paths in the stress – suction space, followed in the experiments. b: Vertical stress vs. measured vertical strain. Square-enclosed numbers indicate the point of flooding of the corresponding specimen. Constitutive model results obtained for stress-suction paths corresponding to tests 3 and 4.
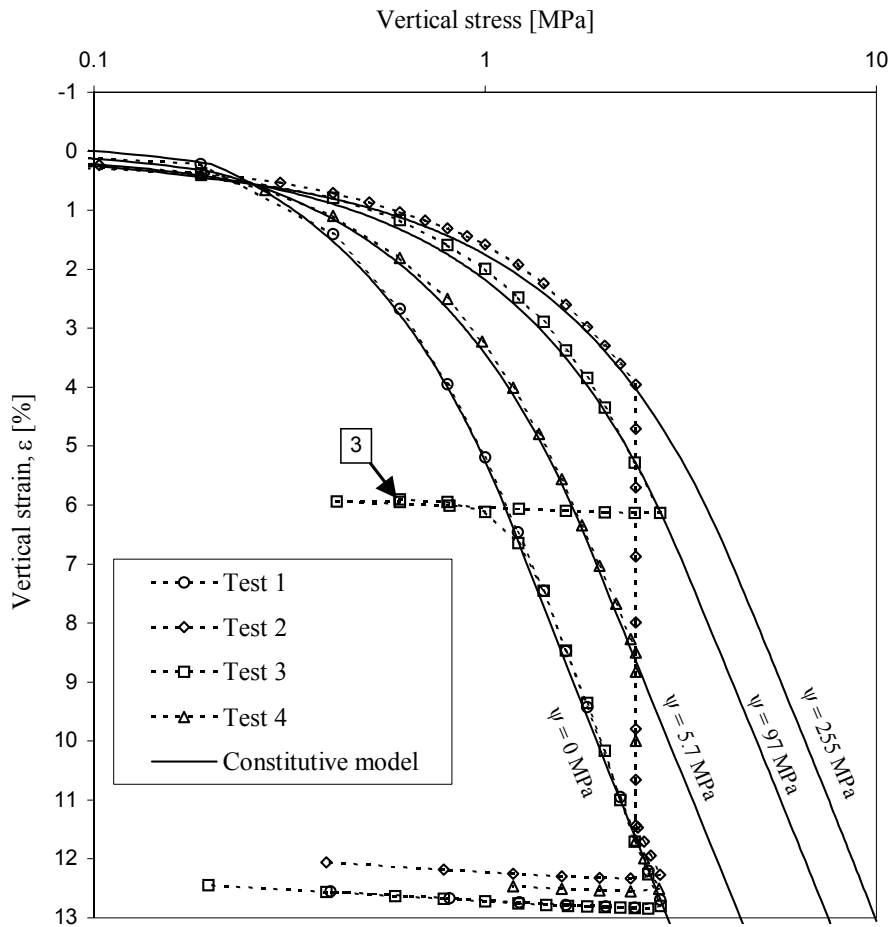
- Figure 12. Experimental results: vertical stress (log scale) vs. measured vertical strain. Square-enclosed numbers indicate the point of flooding of the corresponding specimen. Model predictions for an extended stress range are also given

4.2 Triaxial Tests

The behaviour in shear was investigated by a new triaxial apparatus, which may test samples up to 25 cm in diameter and 50 cm in height under suction controlled conditions. Figure 13 shows a schematic layout of the system.

The cell has a double-walled chamber to allow for a direct measurement of sample volume changes. For redundancy, horizontal strains could also be measured by means of specially developed sensors for diameter changes. Vertical load on the sample and axial displacements are also recorded by means of a load cell and LVDTs located inside the cell. The LVDTs measure the displacement of the upper polished stainless steel loading plate in direct contact with the sample. No bedding errors associated with the penetration of grains into membranes or the compressibility of lubricating grease, reported in other cases (Dendani et al, 1988), are expected here because of the direct contact of the steel plattens and the sample.

Total suction is controlled by means of a closed loop circuit, which induces a vapour flow through the sample. Air relative humidity is imposed by circulating the flowing air through acid or salt solutions at a predetermined concentration. Suction changes are induced by changing the solute concentration. In the tests reported here on "dry" samples the low relative humidity was controlled with a solution of Sodium hydroxide, $Na(OH)_2$. RH was also measured by means of a hygrometer sensor located in the air circuit. Therefore two independent indications of the imposed RH are available. Errors in the determination of RH, due to the precision of both techniques is similar : 1% to 2% of the measured value (Oldecop, 2000). In terms of suction, the error is high (20%-30%) for the low suction range (3 to 10 MPa and smaller (2% - 3%) for a high suction range (100-300MPa). However, mechanical effects induced by suction on granular aggregates tend to depend on the logarithm of suction and therefore a limited mechanical effect of the error in the determination of RH should be expected.

The system has a number of additional features, which have been indicated in figure 13. Confining stresses as high as 2.5 MPa can be applied to samples. The vertical stress may reach a maximum value of 18.5 MPa.

Two test series are reported here to illustrate the behaviour of the gravel. The first series was performed under fully saturated conditions. Once compacted, samples were confined under 0.1, 0.3, 0.5 and 0.8 MPa and then sheared under constant lateral stress, σ_3. (Figure 17). In a second series, samples compacted in a similar manner were maintained at a constant low relative humidity (RH = 36%, equivalent to a total suction s = 142 MPa). Similar stress paths were then applied to the dry samples (Figure 18). Tests on saturated samples are named S1, S3, S5 and S8. The number refers to the intensity of the confining stress. In a similar manner, the three tests performed on "dry" samples are marked as D1, D3, D5 and D8. Grain size distributions were measured for the following states: original material, after compaction, and after the performance of the triaxial tests. They are indicated in Figure 14a and 14b for saturated and "dry" conditions respectively. The application of a dry environment (RH=36%) reduces markedly the particle breakage induced by the stress application

Measured deviatoric (q = σ_1 - σ_3) vs. axial strain (ε_1) response and volumetric deformations vs. axial strain are plotted in Figure 15 for the saturated samples. Unloading-reloading cycles were imposed at some strain levels to estimate the elastic stiffness of the material. Samples were taken to large deformations in an attempt to approximate critical state conditions.

The saturated sample tested under σ_3 = 0.1 MPa (figure 15) shows a marked dilatant behaviour from the beginning of the test. The application of higher confining loads delays the development of dilatancy to higher vertical strains (7 % for σ_3 = 0.3 MPa; 12 % for σ_3 = 0.5 MPa). The sample tested under σ_3 =0.8 MPa shows a compressive behaviour along the test. The application of

suction (Figure 16) increases the measured strength and enhances the dilatant behaviour of the gravel.

The effect of applied suction is now clearly observed comparing the figures 15 and 16, plotted at the same scale. It is also interesting to note that the deviatoric behaviour for saturated and "dry" conditions is similar at low strains.

Significant dilatancy rates were observed at the end of most of the tests performed, as shown in Figures 15 and 16. In all cases samples deformed in a barrel-like shape. The question of the appropriateness of critical state for this gravel samples is therefore difficult to elucidate on the basis of the triaxial tests performed. However, the concept provided a useful framework to interpret the data and to formulate the constitutive model
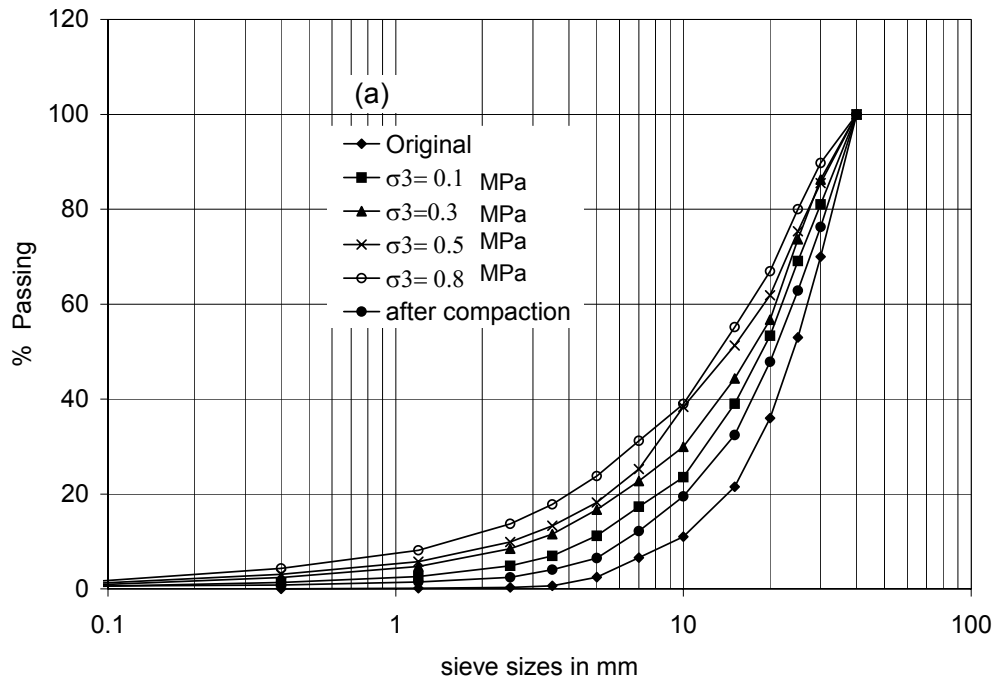
Vectors of incremental plastic strain ($\dot{\varepsilon}_q^p = \frac{2}{3}\left(\dot{\varepsilon}_1^p - \dot{\varepsilon}_3^p\right); \dot{\varepsilon}_p^p = \dot{\varepsilon}_1^p + 2\dot{\varepsilon}_3^p$) have been plotted along the stress paths (Figs. 17 and 18). Plastic strains were derived from total strains by substracting the calculated elastic strains for the considered stress increment. Elastic parameters (E, ν) were derived from the response of the sample in the unloading-reloading paths imposed in tests. Plastic strains develop at the start of the deviatoric stress path. Lines of constant ratio η = q/p ($p = 1/3\left(\sigma_1 + 2\sigma_3\right); \quad q = \sigma_1 - \sigma_3$) have also been plotted in Figures 17 and 18. It appears that plastic strains may be linked to changes in stress ratio η, as it is observed in sands. Yield loci described by q/p = η seem therefore to be a natural choice to describe deviatoric-induced yield. The plots in figures 17 and 18 also indicate the curved nature of strength envelope. In general all the samples tested behaved in a ductile manner.

Yield along Ko lines was clearly demonstrated in the oedometer tests reported before. In fact, yield was observed at the very beginning of deformation in the oedometer tests performed. Compaction does not result in a well defined initial yield locus so that an elastic state could be defined in the stress space. It was checked that, once compacted, any subsequent loading immediately induces plastic strains. The implication of these results is that the yield locus cannot be represented only by the deviatoric lines (η = constant). A "cap" that accounts for yield in compression is also necessary. The important effect of RH on all aspects of stress strain behaviour (stiffness, dilatancy, critical states, particle breakage) is well identified in the tests performed. Further discussion on the effect of RH on shear behaviour of gravel-like material is given in Chavez and Alonso (2003)
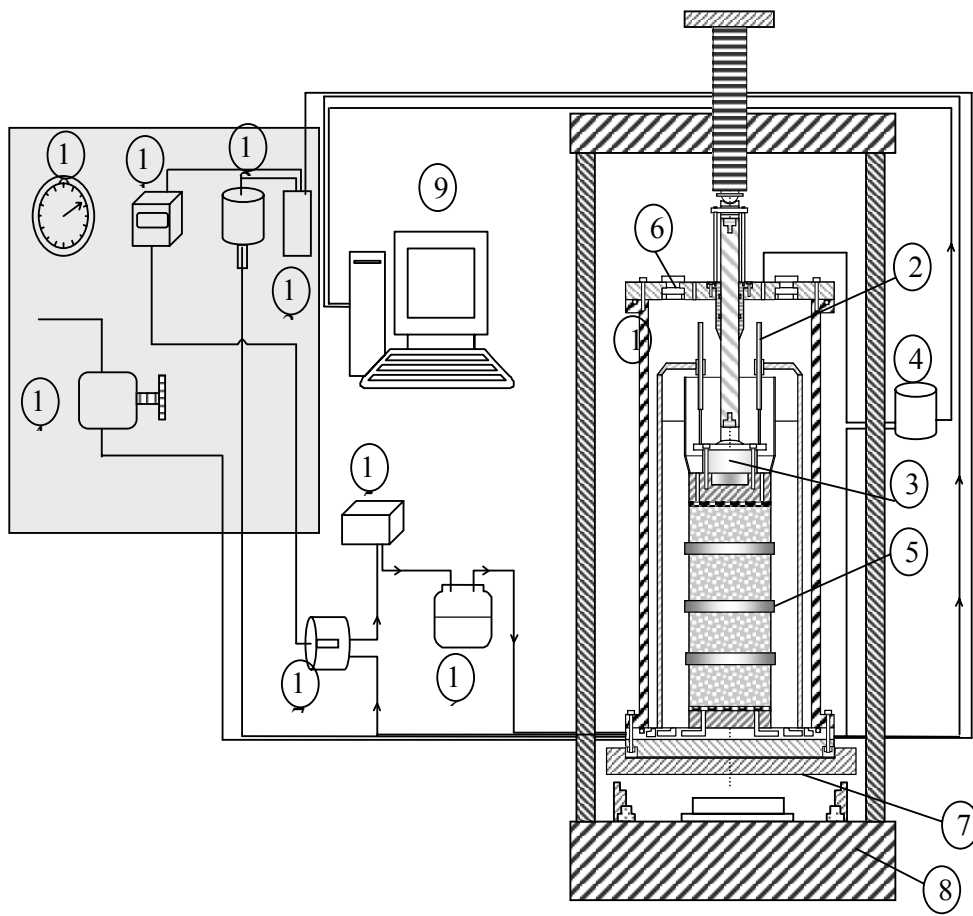
|	
1. Triaxial chamber.	10. Vacuum gage.
2. LVDT for axial measure.	11. Hydrometer.
3. Load cell.	12. Pressure transducer.
4. DPT.	13. Power supply.
5. Diametral Measure Transducer (DMT).	14. Pressure regulator.
	15. Air bomb.
6. Window.	16. Pot with salt solution.
7. Car to move the cell.	17. Hygrometer sensor.
8. Load frame.	
9. Data acquisition system.	

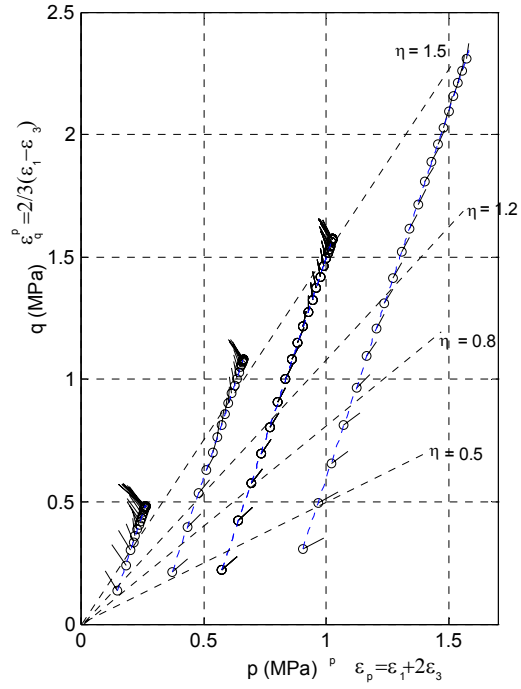- Figure 13. Scheme of the triaxial equipment for large diameter samples under relative humidity control.
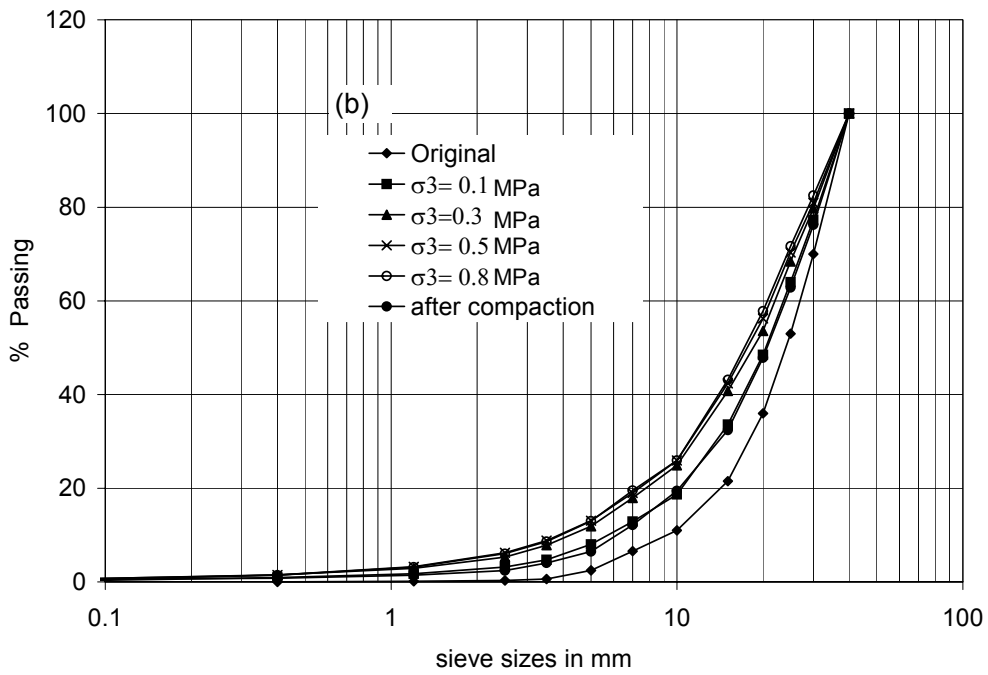
Figure 14. Grain size distributions of specimens tested. a) Saturated samples b) Samples at RH=36%
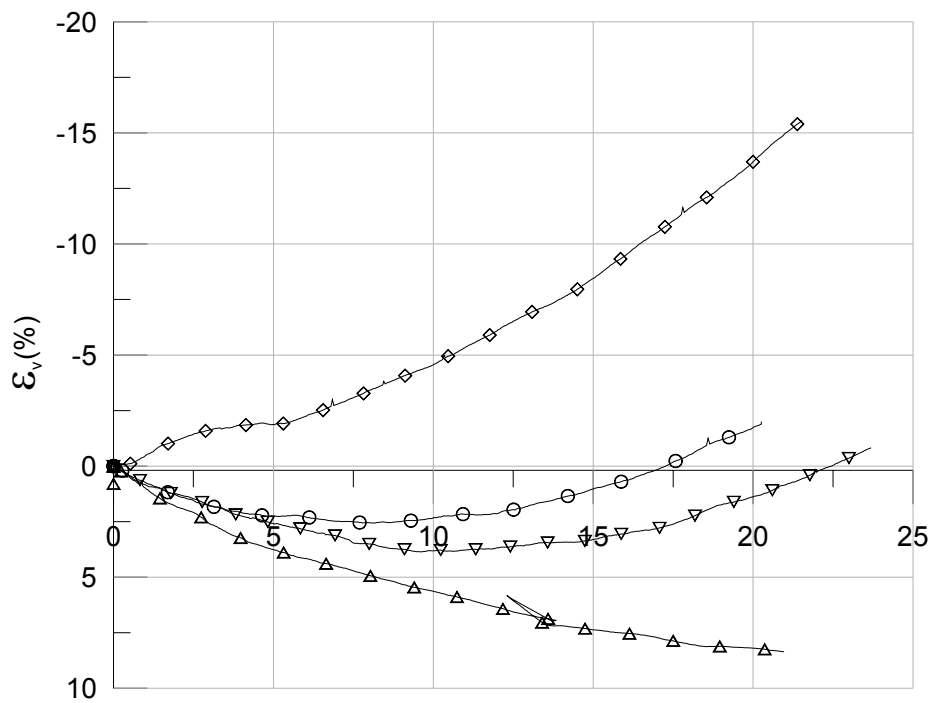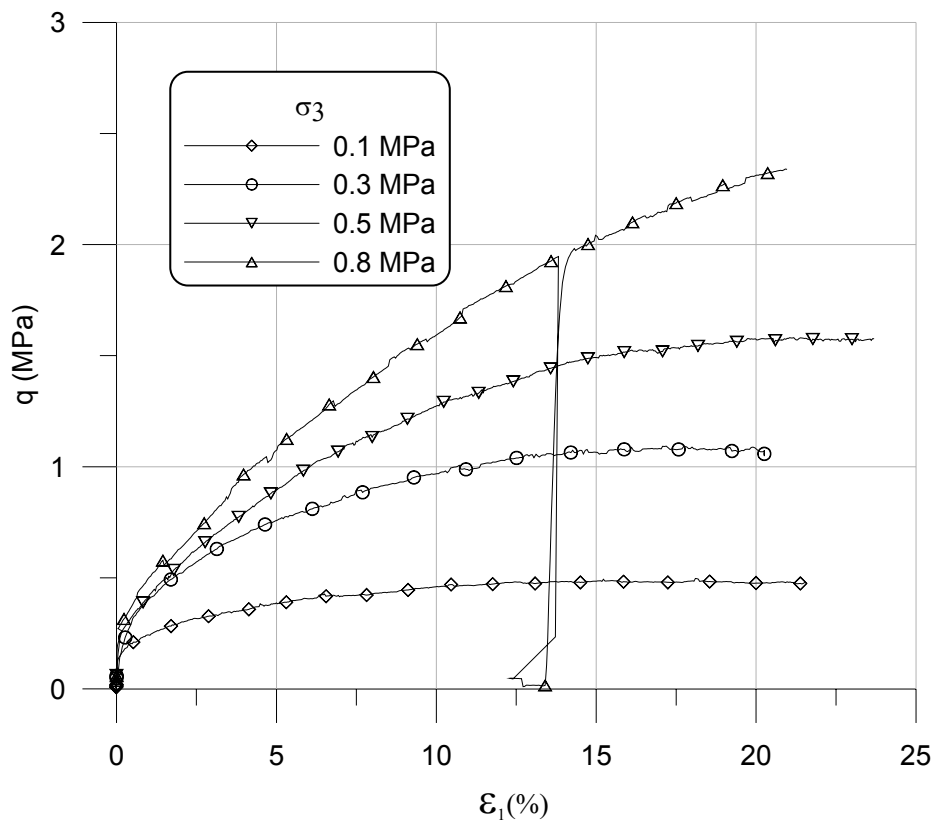
Figure 15. Results of saturated triaxial compression tests on Pancrudo gravel
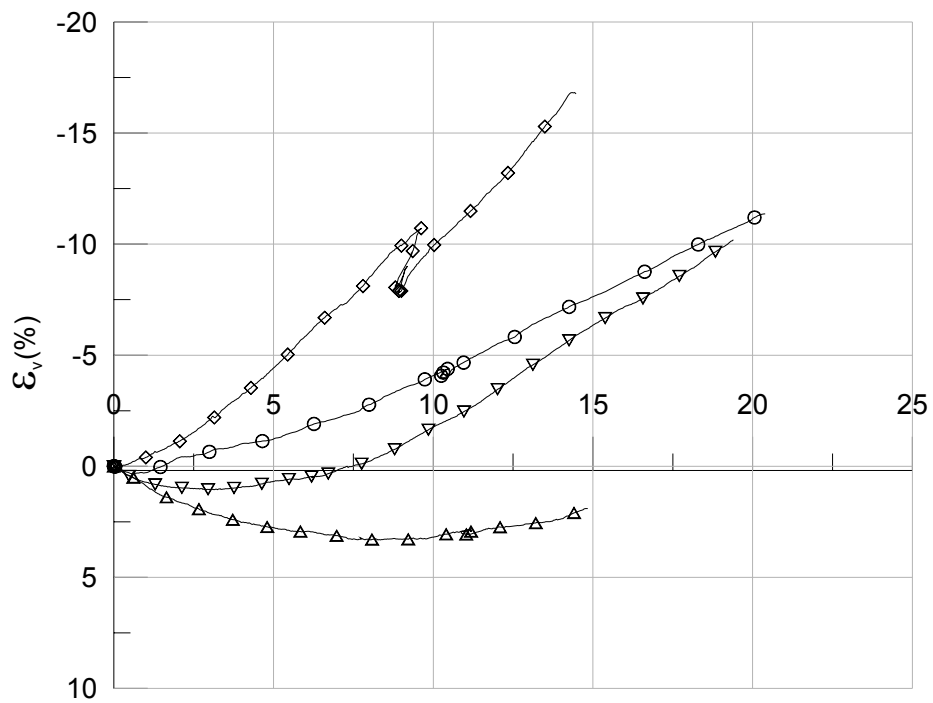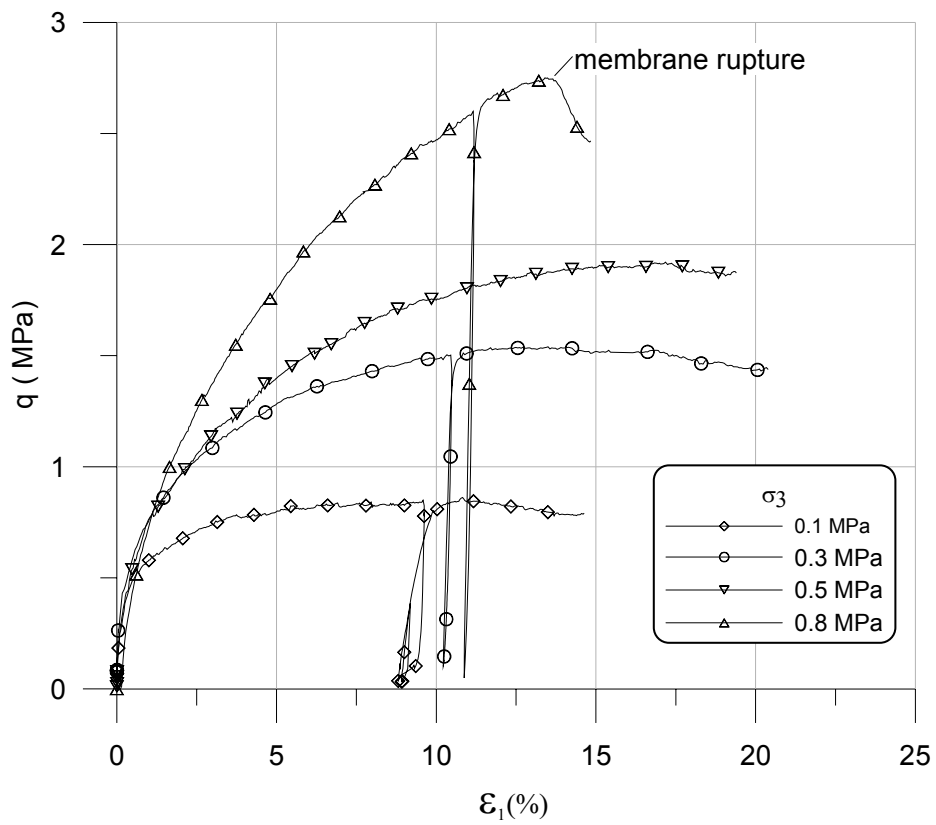
Figure 16. Results of triaxial compression tests on Pancrudo gravel at a RH=36%

Figure 17. Stress paths of saturated triaxial tests on Pancrudo gravel. Also shown are the vectors of incremental plastic strain
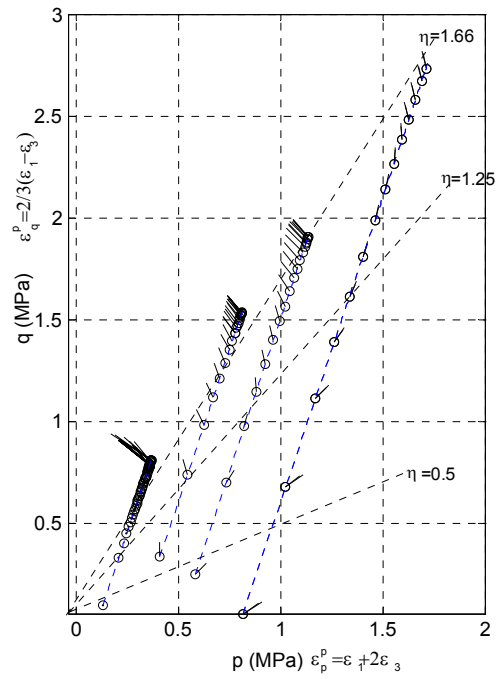
Figure 18. Stress paths of triaxial tests on Pancrudo gravel at RH=36%.Also shown are the vectors of incremental plastic strain

5   CONSTITUTIVE MODELLING

Constitutive modelling of rockfill including suction effects has been presented in several recent papers (Oldecop and Alonso, 2001, 2003; Chavez and Alonso, 2003). In all cases hardening plasticity is used as a general framework and rockfill deformations are interpreted as a combination of particle rearrangement and particle breakage. Both, stress level and Relative Humidity, control particle breakage. This underlying phenomenon explains the influence of suction, which virtually affects all the macroscopic constitutive behaviour.

The third reference provides the most complete formulation. Yielding is described by two yield surfaces: deviatoric and isotropic or "cap" surface. Rockfill degradation (through particle breakage) was made dependent of an effective plastic work which was defined as the difference between total plastic work and the plastic work employed in particle rearrangement.

The isotropic or "cap" behaviour is a fundamental feature of rockfill behaviour and an elastoplastic compressibility behaviour will be described here on the basis of the work reported in Oldecop and Alonso (2003). The three stages of deformation identified in the oedometer tests will be reviewed here.

The particle rearrangement stage ($\sigma_0 < \sigma_y$) is considered separately from the following stages, by means of an independent compressibility index, $\underline{\lambda}^r$, a model parameter. The incremental strain-stress relationship is:

$$d\varepsilon = \underline{\lambda}^r d\sigma_0, \text{ for } \sigma_0 < \sigma_y \tag{5}$$

where $d\varepsilon$ is the total strain increment (elastic plus plastic components) and $d\sigma_0$ is the vertical stress increment. Elastic strain increments may occur due to changes in stress or in suction. The following expressions are assumed to give such elastic increments:

$$d\varepsilon^e = \underline{\kappa}\, d\sigma \tag{6}$$

$$d\varepsilon^\psi = \kappa_\psi\, \frac{d\psi}{(\psi + p_{atm})} \tag{7}$$

where $\underline{\kappa}$ is the elastic stress-related compressibility index, which is assumed to be independent of water action, κ_ψ is the elastic suction-related swelling/retraction index, which is assumed to be independent of the stress level and p_{atm} is the atmospheric pressure. Since, during particle rearrangement, suction changes do not produce plastic strains, the yield surface should be a vertical line in the stress-total suction space:

$$F(\sigma, \psi) = \sigma_0 - \sigma_0{}^* = 0, \quad for\, \sigma_0 < \sigma_y \tag{8}$$

where $\sigma_0{}^*$ is the hardening parameter. A physical interpretation of this hardening parameter will

arise from the model formulation. The hardening rule becomes:

$$d\sigma_0{}^* = \frac{d\varepsilon^p}{\underline{\lambda}^r - \kappa}, \quad \text{for } \sigma_0{}^* < \sigma_y \tag{9}$$

During the clastic yielding stage ($\sigma_0{}^* > \sigma_y$) the compressibility index, $\underline{\lambda}$ should be a function of suction (Figure 10):

$$d\varepsilon = \underline{\lambda}(\psi)\, d\sigma_0 \tag{10}$$

The experimental data suggests the following expression for $\underline{\lambda}(\psi)$:

$$\underline{\lambda}(\psi) = \underline{\lambda}_0 - \alpha_\psi \; Ln\left(\frac{\psi + p_{atm}}{p_{atm}}\right) \tag{11a}$$

and

$$\underline{\lambda}(\psi) \ge \underline{\lambda}^i \tag{11b}$$

where $\underline{\lambda}_0$, $\underline{\lambda}^i$, y α_ψ are model parameters. $\underline{\lambda}_0$ is the maximum compressibility index corresponding to the saturated material ($\psi = 0$). $\underline{\lambda}^i$ has the meaning of a minimum compressibility index. Oldecop & Alonso (2001) hypothesised that a minimum value for the compressibility index would be attained by extreme drying (i.e. under a very high suction), calling it the very dry state. Such a very dry state could not be reached in the experimental program reported before, although a high suction value was imposed to specimen 2 ($\psi = 255$ MPa). However, from a practical point of view, the very dry state can be conventionally defined as a high enough suction value, so as to ensure that it will not be exceeded during the loading path considered in the analysis.

The expression for the yield surface and the hardening rule in clastic yielding can be derived as shown by Oldecop & Alonso (2001):

$$F(\sigma, \psi) = \sigma_0\left[\underline{\lambda}(\psi) - \underline{\kappa}\right] - \sigma_y\left[\underline{\lambda}(\psi) - \underline{\lambda}^i\right] - \sigma_0{}^*\left(\underline{\lambda}^i - \underline{\kappa}\right) = 0 \tag{12}$$

$$d\sigma_0{}^* = \frac{d\varepsilon^p}{\underline{\lambda}^i - \kappa}, \quad \text{for } \sigma_y < \sigma_0{}^* < \sigma_0{}^{ch} \tag{13}$$

where $\sigma_0{}^{ch}$ will be defined immediately.

The experimental data (figures 11 and 12) suggest that the initiation of the clastic hardening stage is marked by a unique value of plastic strain. This is to be expected since the type of mechanical behaviour is determined by the actual configuration of the granular structure and the plastic (volumetric) strain can be considered as a parameter measuring that configuration. Defining a threshold strain value is equivalent to defining a threshold value for the hardening parameter, $\sigma_0{}^*$, in view of eq. (13). Hence, an additional parameter is introduced, $\sigma_0{}^{ch}$, defined as the value of the

39

hardening parameter which marks the onset of clastic hardening. In order to extend the model into the clastic hardening stage, the yield surface is kept the same as in clastic yielding (eq. 12) while the following hardening rule is proposed:

$$d\sigma_0^* = \frac{\sigma_0^* - \sigma_y}{\sigma_0^{ch} - \sigma_y} \frac{d\varepsilon^p}{\underline{\lambda}^i - \underline{\kappa}}, \text{ for } \sigma_0^* > \sigma_0^{ch} \tag{14}$$

The shape of the yield surface in the stress suction space is shown in figure 19, for different values of plastic vertical strain.

A complete set of model parameters is determined on the basis of tests 1 and 2. The very dry state is conventionally defined as the first loading condition of specimen 2 after drying to ψ^{vd} = 255 MPa. The adjustment of linear functions to the normal compression lines in the clastic yielding stage, for the very dry state (test 2) and the saturated state (test 1), respectively, yields the minimum compressibility index, $\underline{\lambda}^i$, and the maximum compressibility index, $\underline{\lambda}_0$. The first loading steps provide the data for the determination of the compressibility index for the particle rearrangement stage, $\underline{\lambda}^r$. The elastic unloading/reloading compressibility index, $\underline{\kappa}$, is computed on the basis of the data obtained during unloading paths. The parameter α_ψ, measuring the variation of the normal compressibility index with suction, is determined by means of equation (11a) for $\psi = \psi^{vd}$ (then $\underline{\lambda}(\psi)$ = $\underline{\lambda}^i$).

The suction related swelling/retraction index is determined on the basis of the heave strain measured in test 1 upon specimen flooding, taking into account equation (7) and the values ψ^{ad} = 97 MPa , $\Delta\varepsilon_{expansion}$ = 0.23% (see fig. 11).
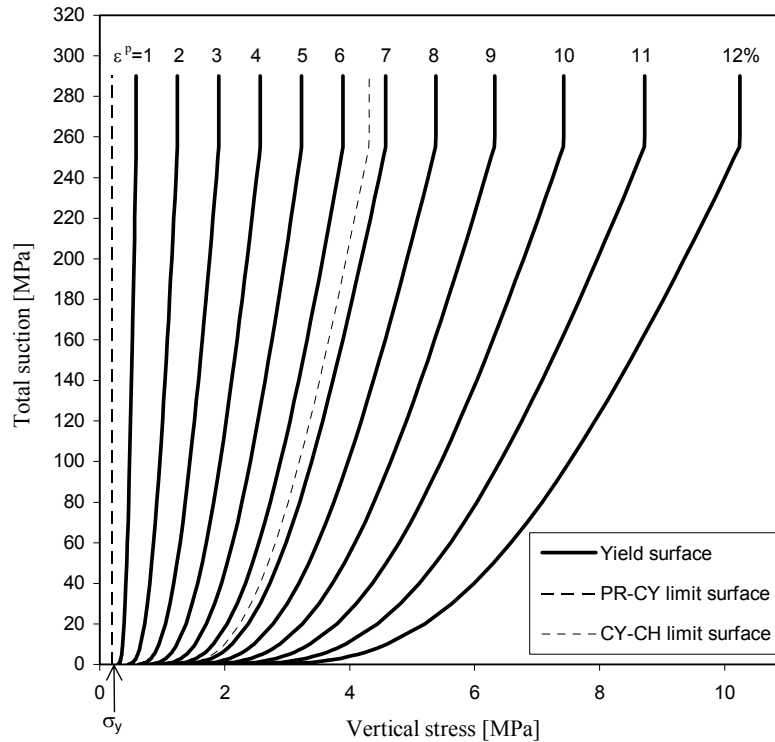
Finally, the threshold value for the hardening parameter marking the onset of the clastic hardening stage, σ_0^{ch}, is derived from the yield surface equation (eq 12). This is done by introducing in eq. 12 the stress-suction values at the point where the stress-strain relationship departs from the straight line and using the previously computed parameters ($\underline{\lambda}^i$, $\underline{\lambda}_0$, $\underline{\kappa}$, α_ψ and σ_y). For test 1, as can be seen in figure 11, the transition point is attained at σ = 1.20 MPa and ψ = 0 MPa.

The computed model parameters are summarised in table 1. Once model parameters were identified, tests 3 and 4 were simulated and compared with observed behaviour (Figures 11b and 12). The agreement is very good.

One of the striking features of the rockfill behaviour is its formal similarity with the behaviour of unsaturated soils of medium to low plasticity and relatively loose structure as described, for instance, in Alonso et al (1987, 1990). Yield surfaces plotted in Figure 19 play formally the same role and have similar shapes to the "Loading-Collapse" (LC) yield curves proposed for unsaturated soils. Yet, the underlying mechanisms and the role of suction are totally different in both cases. A comparison of soil and rockfill behaviour will be presented later.

Table 1. Model parameters determined on the basis of experimental data obtained in tests 1 and 2.

|	
$\underline{\lambda}^r$ [MPa^{-1}]	$2.200{\times}10^{-2}$
$\underline{\lambda}^i$ [MPa^{-1}]	$1.605{\times}10^{-2}$
$\underline{\lambda}^d_0$ [MPa^{-1}]	$6.305{\times}10^{-2}$
α_ψ [MPa^{-1}]	$0.599{\times}10^{-2}$
σ_y [MPa]	0.2
$\underline{\kappa}$ [MPa^{-1}]	$0.092{\times}10^{-2}$
κ_ψ [MPa^{-1}]	$0.033{\times}10^{-2}$
σ_0^{ch} [MPa]	4.310

- Figure 19. Yield surfaces, corresponding to different plastic strain levels. Limit surfaces are shown between particle rearrangement (PR) and clastic yielding (CY) stages and between clastic yielding and clastic hardening (CH) stages.

6   MODELLING ROCKFILL EMBANKMENTS AND DAMS

The very high permeability of a rock fill makes it extremely unlikely in practice a condition of saturated flow. In a zoned earth and rockfill dam the upstream shoulder becomes inundated when the water reservoir level is increased. The downstream shoulder is, however, typically subjected to rainfall infiltration (and evapotranspiration) from and towards the atmosphere.

Similar hydraulic boundary conditions are expected in rockfill embankments used in highway or railway construction. The large open voids of the rockfill remain therefore essentially filled with air and water vapor during the lifetime of these structures. As illustrated in Figure 20, liquid water flow is likely to develop as a film transport mechanism around the large rock blocks. If the rock blocks are not fully saturated water may also penetrate into the particles through the connected porosity and also along cracks. Especially relevant for the purposes of rockfill deformation are the cracks which develop at the particle contacts.

A simplified framework for this complex transport mechanism could be established by postulating two energy states of the rockfill water: the energy associated to the state of the water in open voids and the water energy inside the rock blocks. The first one will control the flow of free water. This free water will be retained by capillary actions at the grain-to-grain contacts and also by rock surface effects. The fundamental mechanisms of water transfer under these circumstances have been discussed, for instance, in Gili and Alonso (2002). In the present work a generalized Darcy type of equation for unsaturated material will be used, instead. It is a simple formulation in which the rate of water transfer is controlled by the bulk degree of saturation through a relative permeability term.
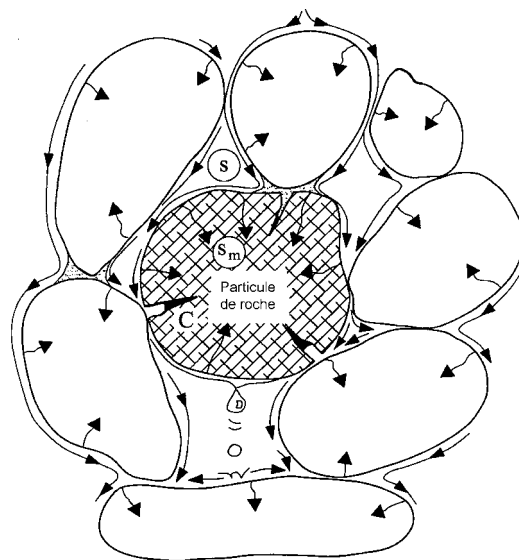
- Figure 20. Scheme to show water transfer in a rockfill.

The local loss of water towards (or from) the rock blocks will be made equivalent to a sink (source) term, which depends on the difference of water energy (or total suction) in the open voids and the rock matrix (s and s_m respectively; see Figure 20). A simple linear formulation for this sink term is therefore:

$$q = -\frac{dw^m}{dt} = -\rho_w \alpha'\left(s - s_m\right)$$

(15)

where q is the flow rate interchanged between the open voids and the rock particles; w^m is the mass of microstructural water (water in the rock particles) and α' is a phenomenological transfer coefficient. If ϕ_m is the porosity of the rock particles, the rate of change of the microstructural mass of water may be also defined as:

$$\frac{dw^m}{dt} = \rho\left(1 - \phi\right)\phi_m \frac{dS_l^m}{dt}$$

(16)

where S_l^m is the microstructral degree of saturation and ϕ is the bulk (or macrostructural) porosity of the rockfill. Water retention properties are also required to complete the formulation. They were determined for the Cambric slate tested under oedometer and triaxial conditions . The following expression may, for instance, define the matrix degree of saturation of the rock particles:

$$S_l^m = \exp\left(-s_m / p_o\right)$$

(17)

where p_o is a reference suction (model parameter).

The coupled flow-deformation problem of the rockfill may be defined through the equations of water mass balance and mechanical equilibrium.

The water mass balance reads

$$\frac{\partial}{\partial t}\left(\theta_l^w S_l \phi + \theta_g^w S_g \phi\right) + \nabla \cdot \left(\mathbf{j}_l^w + \mathbf{j}_g^w\right) = f^w = q$$

(18)

In this expression, ϕ is the rockfill porosity, θ_{lw} and θ_{gw} are the masses of water per unit volume of liquid and gas respectively; $S_g = 1 - S_l$ and $\mathbf{j}_{lw}$ and $\mathbf{j}_{gw}$ are the flow rates (both diffusive and advective of water in liquid and gas phases. The term f^w describes the external supply of water and, in our case it will be represented by the local sink term q as given in equation (18).

The stress equilibrium may be expressed in terms of total stress components, σ, and body forces, b, as:

$$\nabla \cdot \boldsymbol{\sigma} + \mathbf{b} = 0$$

(19)

Internal capillary stress components are assumed to be negligible and therefore formulations used

43

for unsaturated soils (Alonso et al. 1988) are not required here.

The set of equations (15), (18) and (19) may be solved provided a number of constitutive relations and equilibrium restrictions are included (Olivella et al. 1994, 1996). For the open void structure of the rockfill the following information must be provided: the generalized Darcy's law for liquid flow transfer, a Fick's law for vapour diffusion transfer and a water retention relationship between bulk degree of saturation and water suction. The local flow (sink/source term) requires the specification of a water retention relationship (such as equation (17)) and the local transfer coefficient α' (equation (15)).

Rock particles do not deform in the model developed. Rockfill deformation, including particle breakage, is represented by the overall macroscopic constitutive equations described before. They may be conveniently described as:

$$d\boldsymbol{\sigma} = \mathbf{D}_{ep}\left(\mathbf{d\varepsilon} - \mathbf{d\varepsilon_o}\left(s_m\right)\right)$$

(20)

where $\mathbf{D}_{ep}$ is the elastoplastic constitutive matrix and $\mathbf{d\varepsilon_o}$ are the strains associated with changes in the particles water content or, its equivalent, the microstructural suction s_m. Expressions for $\mathbf{D}_{ep}$ and $\mathbf{d\varepsilon_o}(s_m)$ may be derived on the basis of the constitutive relations presented before.

The formulation outlined above has been implemented into an existing numerical tool for thermo-hydro-mechanical analysis of unsaturated/saturated porous media (CODE_BRIGHT). Details of the theoretical basis and numerical formulation of this code may be found in Olivella et al. (1994, 1996). Macrostructural suction is selected as the independent suction variable. At every time increment, s_m may be determined locally through equations (15) and (16).

The capabilities of this formulation were investigated in a simulation of the behaviour of the 40m high shale embankment (Figure 5). No tests were available on the shaly material of this rockfill embankment but a comprehensive testing program was available in a similar material: the Pancrudo shale gravel which has been reported in Chapter 4 of this paper. Therefore, it was decided to simulate the behaviour of a 40m high "column" (the problem was made 1-D for simplicity) of the Pancrudo material subjected to the actual rainfall record measured "in situ" during the period (1993-1997) (Figure 21). Mechanical parameters for the mechanical model have been given in table 1. Water retention properties, permeability and transfer coefficients were derived from the analysis of the oedometer tests performed. The computed settlement rates are plotted in Figure 22 against the actual recorded values. The computed response tend to be faster than the actual measurements but the calculated values reproduce well the effect of rainfall peaks on the velocity of embankment settlement. The total settlement (Figure 23) is underestimated although this is not a very significant result in this case since no tests on the actual embankment material were available. An additional factor in this regard is the fact that no true time effects were introduced into the analysis. Time effects are only a consequence of the evolution of rainfall. Note

also that the high rain intensity at the end of 1996 does not produce a significant increase in settlement rates. The model reproduces well this change in trend. The explanation for this qualitative change is given in Figure 24. At the end of the simulation period the relative humidity prevailing in pores and rock particles of the embankment has increased substantially (suction has decreased steadily) and most of the collapse potential has disappeared. Within the framework of the model developed, the yield curves (shown in Figure 19) have moved towards the right, "pushed" by the stress-decreasing suction increasing the elastic domain. Further wetting is no longer capable of inducing volumetric deformations.

A final interesting aspect of the analysis is shown in Figure 25 were the computed settlement profiles are plotted for several dates. Settlements develop in the lower part of the embankment but not in the upper part. This is a consequence of the threshold effect incorporated into the model through the parameter σ_y . For vertical stresses below σ_y , no collapse effects are induced. This is a consequence of the underlying fracture propagation model which is not active below a given toughness. Within the framework developed σ_y defines an embankment thickness were no water – induced collapse is to be expected. The embankment had no extensometers installed and no comparison with field measurements is possible in this case but Figure 26 shows the settlement records measured in cross-arm D-2 of El Infiernillo dam (the position is shown in Figure 4). No deformations were essentially recorded in the upper parts of the dam, a behaviour which is consistent with the proposed ideas.
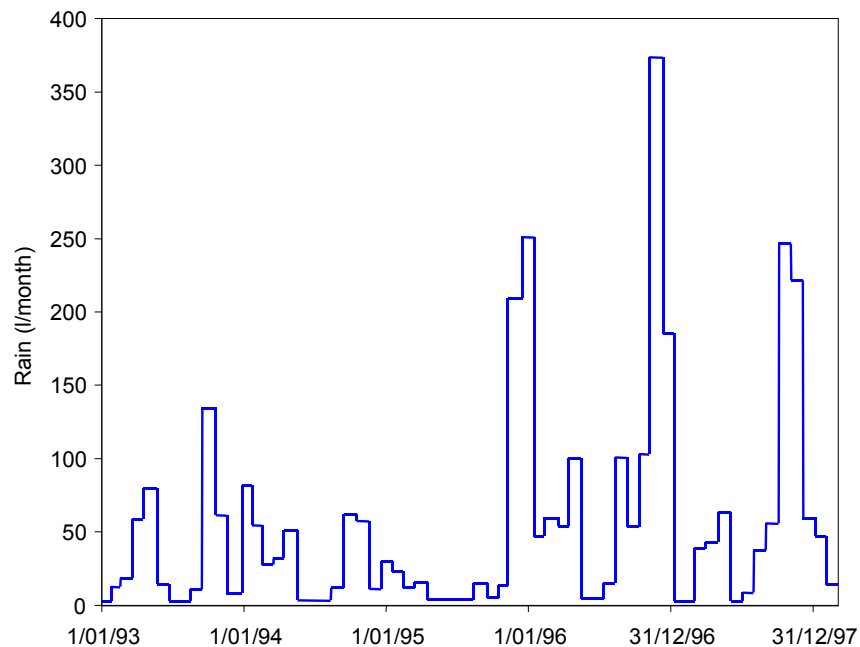

- Figure 21. Rainfall record at the location of a 40 m high shale embankment belonging to the high speed railway line between Madrid and Sevilla (Soriano and Sánchez, 1999)
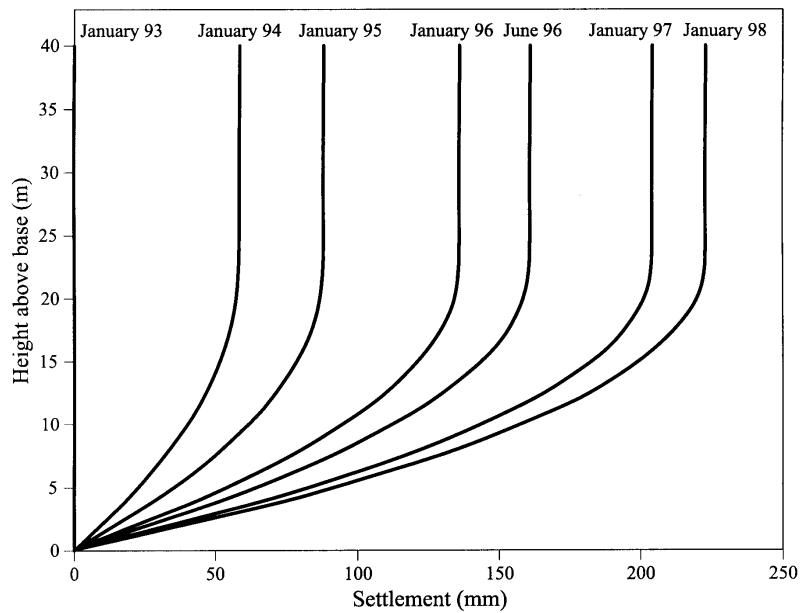
45
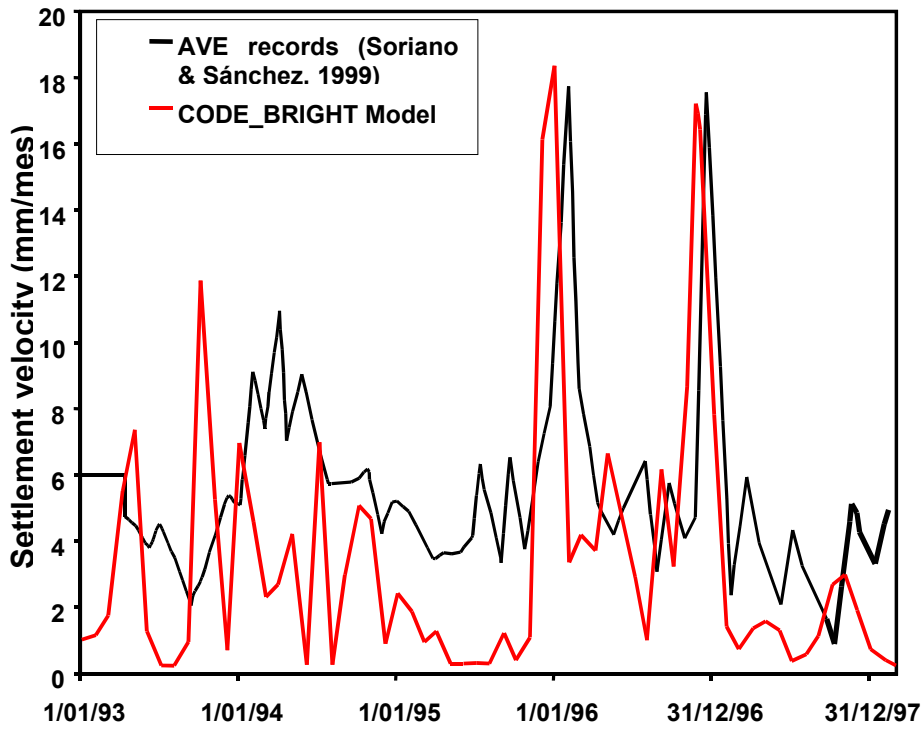
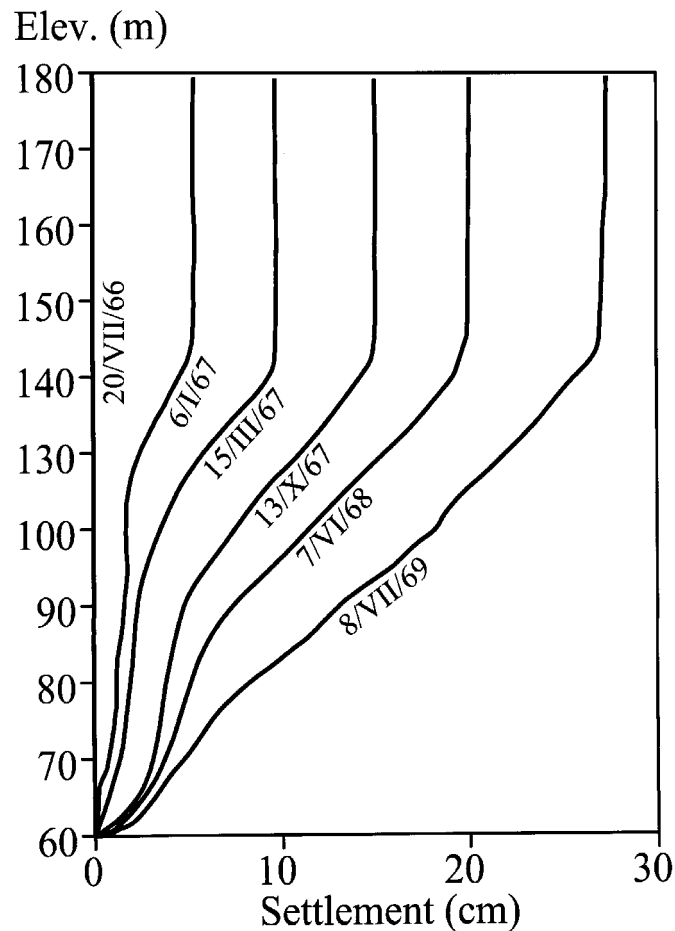- Figure 22. Comparison of measured and computed settlement rates of a 40 m high shale embankment.
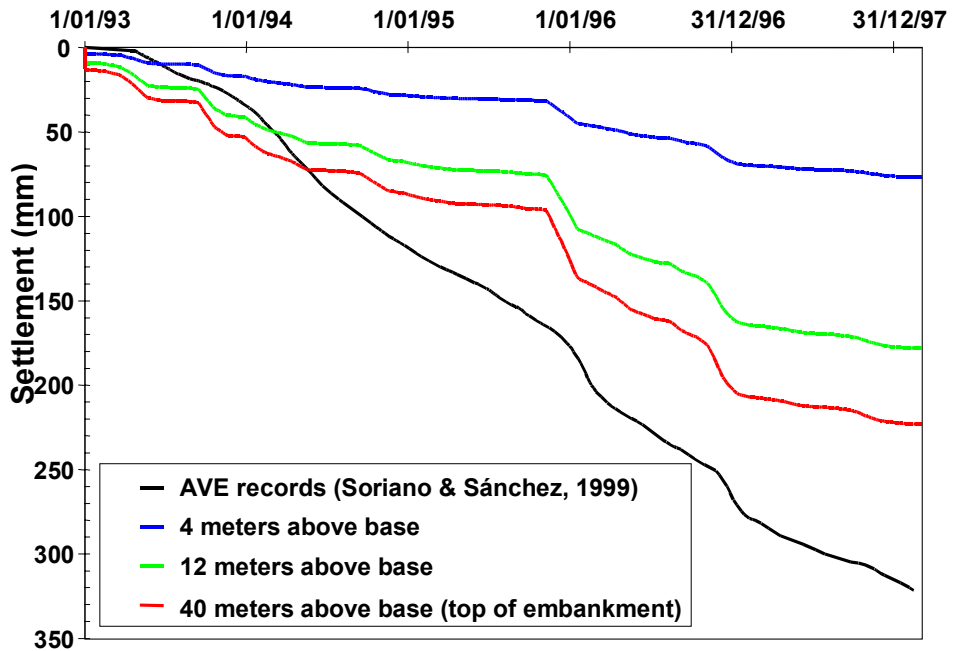
- Figure 23. Measured total settlements and computed values at some elevations within the embankment
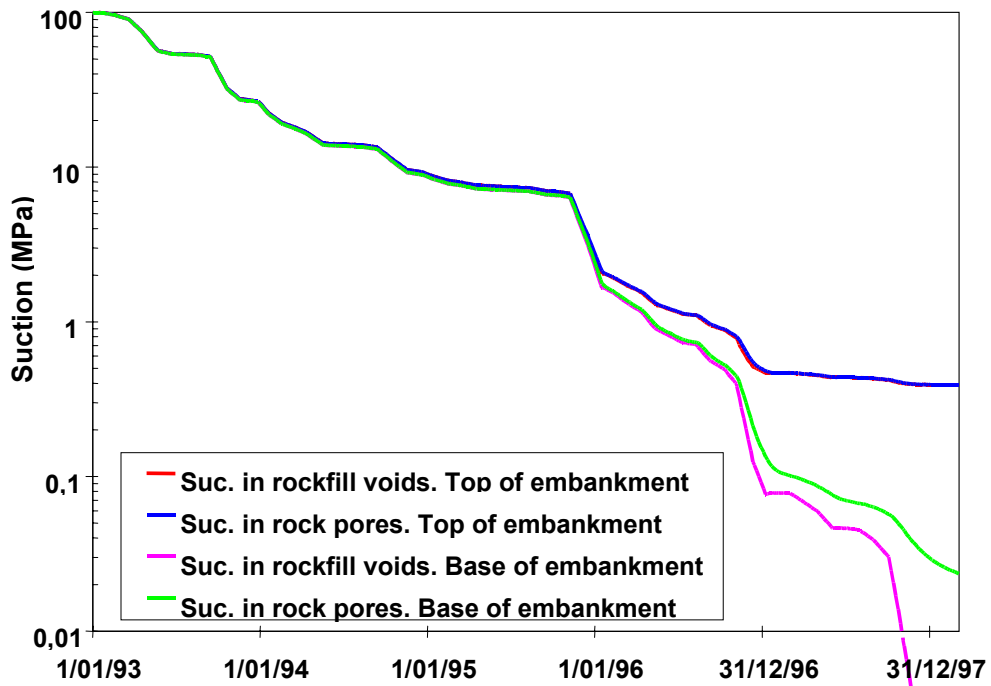
- Figure 24. Computed evolutions of suction at the top and base of the rockfill embankment

- Figure 25. Computed profiles of embankment settlement at several times.

Figure 26. El Infiernillo dam. Measured settlement profiles in cross arm D-2 (Marsal et al, 1976)

7 CONCLUDING REMARKS

A subcritical crack propagation mechanism provides a convenient framework to develop a macroscopic constitutive model for rockfill materials. The model includes the effect of relative humidity changes on rockfill behavior. Laboratory tests as well as field observations demonstrate that humidity changes have a relevant effect on rockfill behavior.

The macroscopic model has been cast in terms of hardening plasticity. It is believed to be the first one to incorporate in a consistent manner water effects on rockfill behavior. The model was first developed for isotropic stress states and later extended to triaxial and general stress conditions. In its simplest form, for isotropic stress conditions, the model is described by six parameters, which may be ideally derived from compressibility tests, in which relative humidity is controlled. More advanced models, including shear hardening have also been developed (Chávez and Alonso, 2003)

Some parallelism between the behavior of moderately active unsaturated soils and rockfill may be found. The elastoplastic model developed by Alonso, Gens and Josa (1990) for unsaturated soils

48

has also formal similarities with the model presented here. However, major differences remain and they have been collected in table 2 to underline the fundamental differences between rockfill and unsaturated soil behavior.

Table 2. Comparison between unsaturated soil and rockfill behavior.

Unsaturated rockfill	Unsaturated soil
Collapse is associated with particle breakage and a subsequent rearrangement of structure	Collapse is associated with particle rearrangement
Particle toughness is a fundamental property	Particle strength does not affect overall behaviour
The effect of suction is to control particle breakage velocity	The effect of suction is to "prestress" soil structure
Particle toughness is included in the model through a single parameter (confining stress, py) For p<py no time delayed deformations exist (no collapse)	There is no equivalent parameter
TOTAL suction controls water induced effects	MATRIC suction controls water induced effects
Time delayed deformations (and hence collapse) is inhibited for very dry states	There is no equivalent concept
Yield stress for the very dry state is conveniently chosen as a hardening parameter	Yield stress of the saturated soil is conveniently chosen as the hardening parameter
Elastoplastic strains (instantaneous and delayed) are linearly related to confining stress for the relevant range of stresses in practice	Elastoplastic stains are linearly related to log (confining stress)
In a compacted material yield starts at zero stress	A compacted material is characterized by an initial yield locus

A further development to the mechanical model comes from the consideration of water transfer mechanisms in rockfill materials. Since wetting or drying the rock particles has a very distinct effect on overall behavior, a procedure to model the local water interchanges has been set out. Particle breakage has been related to the suction or water energy prevailing inside rock particles. The coupled flow-deformation model presented provides a comprehensive tool for the analysis of rockfill structures subjected to environmental changes as well as mechanical loading. Comparison of model calculations and some field observations show encouraging similarities.

8   REFERENCES

Alonso, E.E., Gens, A. & Hight D.W. (1987). Special Problem Soils. General Report. Eur. Conf. On Soil Mech. And Found. Engng. Dublin.

Alonso, E.E., F. Batlle, A. Gens & A. Lloret (1988). Consolidation analysis of partially saturated soils. Application to earthdam construction. Proceedings of the 6th Int. Conf. on Num. Meth. in Geomech. Innsbruck: 1303-1308.

Alonso, E.E., A. Gens & A. Josa (1990). A constitutive model for partially saturated soils. Géotechnique. 40: 405-430.

Alonso, E.E. & L.A. Oldecop (2000). Fundamentals of rockfill collapse. 1st Asian Conference on Unsat. Soils. Singapore.

Alonso, E.E. and Romero, E. (2003) Collapse behaviour of sand. Proc. Of the 2nd Asian Conference on Unsaturated Soils. Osaka, Japan, 325-334.

Atkinson, B. K. & Meredith, P. G. (1987). The theory of subcritical crack growth with applications to minerals and rocks. Fracture Mechanics of Rock, B. K. Atkinson, ed. London: Academic Press Inc., 111-166.

Bernier, F., Volckaert, G., Alonso, E. and Villar, M. (1997), "Suction controlled experiments on Boom Clay," Engineering Geology, Vol. 47, pp. 325-338.

Chávez and Alonso, E.E. (2003) A constitutive model for crushed granular aggregates which includes suction effects. Soils and Foundations, Vol. 43, No. 4, 215-228.

Clements, R. P. (1981). The deformation of rockfill: inter-particle behaviour, bulk properties and behaviour in dams.Ph.D. Thesis, Faculty of Engineering, King´s College, London University.

Coop, M.R. & I.K. Lee (1995) The influence of pore water on the mechanics of granular soils. Proc. 11th ECSMFE, Copenhagen. Vol.1, 1.63-1.72.

De Alba, E. & Sesana, F. (1978). The influence of expansive minerals on basalt behaviour. Proc. Int. Congress Engng Geology, Madrid: 107-116.

Delage, P., Howat M. D. and Cui, Y. J. (1998). "The relationship between suction and swelling properties in a heavily compacted unsaturated clay," Engineering Geology, Vol. 50, pp. 31-48.

Delgado, J., Veiga Pinto, A. & Maranha das Neves, E. (1982). Rock index properties for prediction of rockfill behaviour. Memoria no. 581, Laboratório Nacional de Engenharia Civil, Lisbon.

Dendani, H., Flavigny, E. and Fry, J.J. (1988). "Triaxial Test for Embankment Dams: Interpretation and Validity". Advanced Triaxial Testing of Soil and Rock, ASTM STP 977, Robert T. Donaghe, Ronald C. Chaney and Marshall L. Silver, Eds., American Society for Testing Materials, Philadelphia, 486-500.

Esteban, F. (1990), Caracterización de la expansividad de una roca evaporítica. Identificación de los mecanismos de hinchamient, Ph. D. Thesis, Universidad de Cantabria, Santander.

Freiman, S.W. (1984). Effects of chemical environment s on slow crack growth in glasses and ceramics. J. Geophysical Research, 89 (B6): 4072-4076.

Gens, A. García Molina, A.J, Olivella, S., Alonso, E.E., and Huertas, F. (1998). Analysis of a full scale in situ test simulating repository conditions. International Journal for Numerical and Analytical Methods in Geomechanics, 22: 515-548

Gens, A. and Alonso, E.E. (1992) A framework for the behaviour of unsaturated expansive clays. Can. Geot. J. 29, 1013-1032.

Gili, J. (1988). Modelo microestructural para medios granulares no saturados. Tesis Doctoral. Barcelona: UPC.

Gili, J. and Alonso, E.E. (2002) Microstructural deformation mechanisms of unsaturated granular soils. Int. Jnl. for Num. And Anal. Meth. In Geomech., 26, 433-468

Marsal, R. J. (1973). Mechanical properties of rockfill. Embankment Dam Engineering. Casagrande Volume. Hirschfeld, R. C. & Poulos, S. J., eds. John Wiley & Sons.

Marsal, R.J., Arellano, L.R.Guzmásn, M.A. & Adame, H. (1976). El Infernillo. Behaviour of dams built in Mexico. Mexico: Instituto de Ingeniería, UNAM.

McDowell, G.R. and M.D. Bolton (1998). On the micromechanics of crushable aggregates. Géotechnique 48, No. 5, 667-679

Michalske, T.A. & Freiman, S.W. (1982). A molecular interpretation of stress corrosion in silica. Nature, 295: 511-512.

Nara, Y. and Kaneko, K. (2003) The dependence of subcritical crack growth in rocks on water vapour pressure. Proc. Of the Int. Conf. On coupled T-H-M-C Processes in Geo-systems: Fundamentals, Modelling, Experiments and Applications. (GeoProc 2003) Part 1:526-531. Stockholm, Sweden.

Nelson, J.D. and Miller, D.J. (1992) Expansive soils. Problems and Practice in Foundation and Pavement Engineering. Wiley

Nobari, E. S. & Duncan, J. M. (1972). Effect of reservoir filling on stresses and movements in earth and rockfill dams. Department of Civil Engineering, Report No. TE-72-1, University of California.

Oldecop, L. (2000). "Compresibilidad de escolleras. Influencia de la humedad". PhD. Thesis. UPC.

Oldecop, L. and Alonso EE (2001). "A model for rockfill compressibility". Géotechnique 51(2), pp. 127-140.

Oldecop, L.A. and Alonso, E.E. (2003), "Suction effects on rockfill compressibility" Géotechnique,

Vol. 53, pp. 289-292.

Olivella, S., J. Carrera, A. Gens & E.E. Alonso (1994). Nonisothermal multiphase flow of brine and gas through saline media. Transport in Porous Media. 15:271-293.

Olivella, S., A. Gens & A. Josa (1996). Numerical formulation for a simulator (CODE_BRIGHT) for the coupled analysis of saline media. Engineering Computations. 13, 7: 87-112.

Pestana J.M.and A.J.Whittle (1995) Compression model for cohesionless soils. Géotechnique, 45, No. 4, 611-631.

Romero, E., (1999), "Thermo-hydro-mechanical behaviour of unsaturated Boom Clay: an experimental study," Ph. D. Thesis, Universitat Politècnica de Catalunya, Barcelona.

Romero, E., Gens, A. and Lloret, A., (1999), "Water permeability, water retention and microstructure of unsaturated compacted Boom Clay," Engineering Geology, Vol. 54, pp. 117-127.

Romero, E., Gens, A. and Lloret, A. (2001) "Laboratory testing of unsaturated soils under simultaneous suction and temperature control". Proc. 15th ICSMGE, Istanbul, vol 1, 619-622.

Sherard, J.L. & Cooke, J.B. (1987). Concrete-face rockfill dam: I. Assessment. J. Of Geotech. Engng. ASCE, 113 (10): 1096-1112.

Soriano, A. & Sánchez, F. J. 1999 Settlements of railroad high embankments. Proc. XII European Conf. on Soil Mech. and Geotech. Eng., Netherlands.

Sowers, G. F., Williams, R. C. & Wallace, T. S. (1965). Compressibility of broken rock and settlement of rockfills. Proc. 6th ICSMFE, 2, Montreal: 561-565.

Terzaghi, K. (1960). Discussion on salt springs and lower bear river dams. Trans. ASCE, 125 (2): 139-148.

Villar, M. (1999), "Investigation of the behaviour of bentonite by means of suction-controlled oedometer tests," Engineering Geology, Vol. 54, pp. 67-73.

Vutukuri, V. S., Lama, R. D. y Saluja, S. S. (1974). Handbook on Mechanical Properties of Rocks, Vol. 1, Trans Tech Publications, Claustahl.

Wiederhorn, S. M., Fuller, E. R. and Thomson, R. (1980), "Micro-mechanisms of crack growth in ceramics and glasses in corrosive environments," Met. Sci., Vol. 14, pp. 450-458.

Wiederhorn, S. M., Freiman, S.W., Fuller, E.R. & Simmons, C.J. (1982). Effects of water and other dielectrics on crack growth. J. Mater. Sci., 17: 3460.

Yahia.-Aissa, M. (1999), "Comportement hydromécanique d'une argile gonflante fortement compactée," Ph. D. Thesis, École Nationale des Ponts et Chaussées, Paris.

Spencer J. Buchanan '26 Professorship in Civil Engineering

Texas A&M University Development Foundation
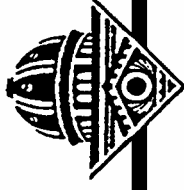
Name *(please print)* _____ Class _____

Address _____

City _____ State _____ Zip _____

Yes, I would lie to make a personal gift to the Buchanan Professorship in the amount of: $ _____

My company, _____, has a matching program and will contribute $ _____

Total Pledge $ _____

Enclosed is my check for $ _____ made payable to the TAMU DEVELOPMENT FOUNDATION with a memo on the check: Buchanan Professorship. Please send to TAMU Foundation, 401 George Bush Drive, College Station, TX 77840

Phone: 979 845-5113   FAX: 979 862-8572   E-Mail: c-wootton@tamu.edu